IL-3 Decreases Cartilage Degeneration by Downregulating Matrix Metalloproteinases and Reduces Joint Destruction in Osteoarthritic Mice

Supinder Kour,* Manasa G. Garimella,* Divya A. Shiroor,† Suhas T. Mhaske,* Snehal R. Joshi,* Kanupriya Singh,* Subhashis Pal,‡ Monika Mittal,‡ Hari B. Krishnan,§ Naibedya Chattopadhyay,‡ Anil H. Ulemale,† and Mohan R. Wani*

Osteoarthritis (OA) is a chronic disease of articular joints that leads to degeneration of both cartilage and subchondral bone. These degenerative changes are further aggravated by proinflammatory cytokines including IL-1β and TNF-α. Previously, we have reported that IL-3, a cytokine secreted by activated T cells, protects cartilage and bone damage in murine models of inflammatory and rheumatoid arthritis. However, how IL-3 protects cartilage degeneration is not yet known. In this study, we investigated the role of IL-3 on cartilage degeneration under both in vitro and in vivo conditions. We found that both mouse and human chondrocytes show strong expression of IL-3R at gene and protein levels. IL-3 increases the expression of mouse chondrocyte-specific genes, Sox9 and collagen type IIa, which were downregulated by IL-1β. Moreover, IL-3 downregulated IL-1β– and TNF-α–induced expression of matrix metalloproteinases in both mouse and human chondrocytes. Interestingly, IL-3 reduces the degeneration of articular cartilage and subchondral bone microarchitecture in a mouse model of human OA. Moreover, IL-3 showed the preventive and therapeutic effects on cartilage degeneration induced by IL-1β in micromass pellet cultures of human mesenchymal stem cells. Thus, to our knowledge, we provide the first evidence that IL-3 has therapeutic potential in amelioration of degeneration of articular cartilage and subchondral bone microarchitecture associated with OA. ***The Journal of Immunology*****, 2016, 196: 5024–5035.**

Osteoarthritis (OA) is a degenerative disease of joints, characterized by progressive loss of cartilage and subchondral bone. Genetic predisposition and environmental factors such as sex, obesity, misalignment, and injuries increase the risk for development of OA (1). These factors cause repeated abnormal mechanical stress at load-bearing joints, leading to its altered biomechanics (2). The origin of OA from cartilage or subchondral bone is not very clear; however, both are interdependent and damage from one subsequently suffuses to the other (3–5).

Cartilage at articular surface aids in smooth mobility of joints with least friction because of tensile strength of matrix secreted by cartilage cells (6). Cartilage is composed of a sparse population of chondrocytes distributed in collagen- and proteoglycan-rich extracellular matrix. Chondrocytes are the first skeleton-specific cell type to appear during embryonic development. They form growth plate in long bones and are of foremost importance in the process of bone formation as they lay the basic framework for longitudinal growth of bones (7, 8). Chondrocytes participate in the synthesis, as well as the degradation, of cartilage matrix and are highly sensitive to pathological changes in the joint microenvironment. Any injury that leads to irreversible physical damage to cartilage induces inflammatory microenvironment in the joints (9, 10). Hypertrophic chondrocytes lose their proliferative potential as well as the property of matrix synthesis, and hence cannot compensate for the cartilage damage (11, 12).

The inflammatory microenvironment at the affected joints attracts immune cells leading to enhanced degeneration of cartilage matrix and bone (13). The proinflammatory cytokines IL-1β and TNF-α are key players in the pathophysiology of OA (14). These cytokines promote the onset of disease and enhance the degenerative processes by stimulating apoptotic and matrix-degrading pathways in affected cartilage (15). Matrix metalloproteinases (MMPs) triggered by proinflammatory cytokines assist in cartilage destruction during arthritic conditions (16).

IL-3, a cytokine secreted by activated T lymphocytes, stimulates proliferation, differentiation, and survival of pluripotent hematopoietic stem cells. It is a broadly acting hematopoietic-regulatory protein, which acts on a number of cell lineages including macrophages, mast cells, neutrophils, eosinophils, and megakaryocytes. Previously, we have documented that IL-3 irreversibly inhibits in vitro osteoclast differentiation induced by receptor activator of NF-κB

*National Centre for Cell Science, Savitribai Phule Pune University Campus, Ganeshkhind, Pune 411007, India; †Department of Veterinary Surgery, Krantisinh Nana Patil College of Veterinary Science, Shirwal 412801, Satara, India; ‡Division of Endocrinology, Council of Scientific and Industrial Research–Central Drug Research Institute, Lucknow 226031, India; and §Department of Orthopaedic Surgery, Armed Forces Medical College, Pune 411040, India

ORCIDs: 0000-0003-0866-7267 (S.K.); 0000-0001-9085-5675 (D.A.S.); 0000-0002-5672-1355 (S.T.M.); 0000-0003-3511-1459 (K.S.); 0000-0001-7901-8569 (H.B.K.); 0000-0003-2473-0246 (N.C.).

Received for publication April 17, 2015. Accepted for publication April 13, 2016.

This work was supported by the Department of Biotechnology under Government of India Grant BT/HRD/34/01/2009 (to M.R.W.), Council of Scientific and Industrial Research, New Delhi, India Grant BSC0201 (to N.C.), and a Senior Research Fellowship from the Council of Scientific and Industrial Research, New Delhi, India (to S.K.).

Address correspondence and reprint requests to Dr. Mohan R. Wani, National Centre for Cell Science, Savitribai Phule Pune University Campus, Ganeshkhind, Pune 411007, India. E-mail address: mohanwani@nccs.res.in

The online version of this article contains supplemental material.

Abbreviations used in this article: ACL, anterior cruciate ligament; BV/TV, trabecular bone volume fraction; Col2a, collagen type IIa; Conn.D, connectivity density; μ-CT, microcomputed tomography; MMP, matrix metalloproteinase; MSC, mesenchymal stem cell; OA, osteoarthritis; OARSI, OsteoArthritis Research Society International; SMI, structure model index; Tb. N., trabecular number; Tb. Pf., trabecular pattern factor.

ligand and TNF-α in both mice and human osteoclast precursors and directs the cells to macrophage and dendritic cell lineages (17–19). We have also shown that IL-3 is a potent inhibitor of pathological bone resorption induced by TNF-α and other proinflammatory cytokines such as IL-1α, TGF-β1, TGF-β3, IL-6, and PGE_2 (20). Recently, we demonstrated that IL-3 has anti-inflammatory activity in vivo and indirectly protects cartilage and bone damage in murine models of inflammatory and rheumatoid arthritis (20, 21). However, the role of IL-3 on chondrocyte differentiation and cartilage degeneration in OA is not yet known.

In this study, we investigated the effect of IL-3 on cartilage degeneration under both in vitro and in vivo conditions. We found that IL-3 upregulates the expression of chondrocyte genes important for matrix synthesis, and downregulates the expression of MMPs under inflammatory conditions in both mouse and human chondrocytes. Interestingly, IL-3 reduces the degeneration of articular cartilage and subchondral bone microarchitecture in mouse model of human OA. Moreover, IL-3 decreases IL-1β–induced matrix degradation in micromass pellets of human mesenchymal stem cells (MSCs). Thus, to our knowledge, we provide the first evidence that IL-3 has a chondroprotective role in OA.

Materials and Methods

Animals

BALB/c mice pups (2–4 d old) and C57BL/6 male mice (8–10 wk old) were obtained from the Experimental Animal Facility of National Centre for Cell Science, Pune, India. Water and food were provided ad libitum. All the protocols involving animal use were approved by an Institutional Animal Ethics Committee.

Collection of human samples

Nondegenerated human cartilage tissues were harvested from femoral condyles after joint replacement surgeries at Armed Forces Medical College, Pune, India. All the protocols followed for harvesting, handling, processing, and disposal of human samples were approved by an Institutional Ethics Committee.

Abs, recombinant proteins, and general reagents

FITC anti-CD123 (IL-3Rα) and its isotype were from BD Biosciences. Abs for Sox9, collagen type IIa (Col2a), and aggrecan were from Santa Cruz. The fluorochrome-conjugated secondary Abs were obtained from Abcam, and HRP-conjugated secondary Abs were from Bangalore Genei. Abs for MMP-3 and MMP-13 and recombinant cytokines such as human IL-3, IL-1β, TNF-α, and TGF-β3 were obtained from R&D Systems. Recombinant mouse IL-3 and IL-1β were obtained from BD Biosciences. DMEM with high glucose (4.5 g/l), FBS, L-glutamine, TRIzol reagent, cDNA synthesis kit, and SYBR Green were obtained from Invitrogen. Chondrogenesis induction media plus bullet kit was from Lonza. Collagenase and dispase were purchased from MP Biomedicals. BrdU incorporation ELISA was obtained from Roche. Bicinchoninic acid kit and ECL picochemiluminescence substrate were purchased from Thermo-Pierce. Total MMP-3 ELISA kit was obtained from R&D Systems, and the assay was performed as per the manufacturer's instructions.

Isolation of mouse and human chondrocytes

Murine chondrocytes were isolated from knee balls (cartilaginous epiphyses of tibia and femur in the tibio-femoral joints) and sternum of mouse pups. Tissues were digested with collagenase (3 mg/ml) at 37°C for 1–2 h for soft tissue removal, followed by second enzyme digestion for 3–4 h for isolation of cells. Cells were washed and cultured in DMEM with high glucose supplemented with 2 mM L-glutamine and 10% FBS.

Human cartilage tissues were digested in medium containing 1% collagenase and 0.2% dispase for 10, 20, 30, 30, 15, and 10 min at 37°C in shaker water bath. The first cell fraction was discarded, whereas rest were pooled, washed, and cultured at a density of $5–10 \times 10^3$ cells/cm^2. The cells were allowed to adhere to plastic surface and were fed every 2 d.

RT-PCR and quantitative real-time PCR

Expression of IL-3Rα, MMP-1, MMP-3, MMP-13, and chondrocyte-specific genes Sox9, Col2a, and aggrecan was assessed by RT-PCR and real-time PCR using primer sequences (IDT) listed in Table I. RNA was isolated from chondrocytes using TRIzol reagent. Total RNA (2 μg) was used to synthesize cDNA by reverse transcription (cDNA synthesis kit). cDNAs were amplified using PCR for 30–35 cycles. Each cycle consisted of 30 s of denaturation at 94°C, 30 s of primer annealing at 60°C, and 30 s of extension at 72°C. GAPDH and β-actin were used as endogenous controls.

For real-time PCR, 10 μl reaction mixture containing SYBR Green and 10 pmol of each primer were used. PCR was set using StepOnePlus system (Applied Biosystems). The PCR program was comprised of 1 cycle of denaturation at 95°C for 10 min and 40 cycles of denaturation at 95°C for 15 s, primer annealing, and extension at 60°C for 60 s, followed by melt curve analysis. Each reaction was run in duplicates. Data were analyzed for fold difference using comparative 2^{-ddCT} method.

Western blotting

Chondrocytes were lysed in proteinase and phosphatase inhibitor containing radioimmunoprecipitation assay–based cell lysis buffer. For isolation of proteins from tissues, operated whole-knee joints were crushed in liquid nitrogen and tissue lysates were collected in radioimmunoprecipitation assay lysis buffer. Supernatant obtained after centrifugation at $12{,}000 \times g$ for 20 min was quantified for total cellular proteins using bicinchoninic acid kit. A total of 40 μg total protein was denatured, subjected to SDS-PAGE (10%), and transferred onto nitrocellulose membrane. Blots were blocked for 30 min in BSA and incubated with primary Ab (1:1000) for 3 h. After washing, the membranes were incubated with HRP-conjugated secondary Ab, and labeled proteins were detected using ECL reagents. Relative intensities for the expression of MMPs were analyzed by densitometry using ImageJ software (National Institutes of Health).

Flow cytometric analysis

Chondrocytes were characterized by flow cytometry using primary Abs specific for Sox9, aggrecan, Col2a, and IL-3Rα. Cells were fixed in 4% paraformaldehyde, followed by blocking of nonspecific binding in BSA. Cells were then incubated with primary Ab (1:50) for 1 h at 4°C. After washing, cells were treated with fluorochrome-conjugated secondary Ab for 1 h in the dark. For intracellular staining, cells were permeabilized using 0.1% Triton X-100 for 15 min. Cells were washed, resuspended in sheath fluid, and acquired on BD FACS Canto II. Cells incubated with fluorochrome-conjugated secondary or isotype Ab were used as nonspecific controls. Data were analyzed using FACS DIVA software (BD Biosciences).

Immunofluorescence microscopy

Coexpression of IL-3Rα and chondrocytic markers was carried out using fluorochrome-conjugated Abs. Chondrocytes cultured on glass coverslips were fixed in 4% paraformaldehyde for 10 min, followed by blocking in BSA. Cells were incubated with primary Ab (1:50) for 4 h, washed, and then incubated with fluorochrome-conjugated secondary Ab for 2 h in the dark. Coverslips were mounted onto glass slides using DAPI-containing mounting medium, and images were acquired using confocal microscope equipped with argon and helium lasers (Zeiss).

BrdU incorporation ELISA

Chondrocytes (5×10^3 cells/well) cultured in 96-well plate were treated for 72 h with different concentrations of IL-3. BrdU incorporation ELISA was performed as per the manufacturer's instructions.

MTT assay

Cells were treated with different concentrations of IL-3. After 72 h, medium was replaced with MTT (0.5 mg/ml). Formazan crystals were dissolved in 100 μl acidified isopropanol, and absorbance was measured at 570 nm.

Micromass pellet culture of human MSCs

Human MSCs were differentiated into chondrocytes using pelleted micromass culture assay (22) with slight modification. In brief, MSCs (2×10^5 cells/well) were seeded in U-bottom 96-well plate and centrifuged at $200 \times g$ for 10 min. The cell pellets were incubated in chondrogenesis induction medium and 10 ng/ml TGF-β3. These cell pellets were half fed every 2 d. After 21 d, cell pellets were fixed in 10% formalin, and 5-μm-thick sections were examined microscopically for the presence of chondrocytes and lacunae by H&E staining and matrix deposition by toluidine blue staining. The images of H&E-stained sections were quantitated for percent matrix and percent matrix degradation using image analysis software ImageJ.

Induction of OA in mice

Mouse model of human OA was developed by surgical transection of anterior cruciate ligament (ACL) as described previously (23) with slight modification. In brief, C57BL/6 male mice 8–10 wk old were anesthetized. A *para*-median skin incision was made on the knee using medial *para*-patellar approach, and patella was retracted laterally. ACL was identified and transected using microsurgical instruments. The surgical wound was closed in layers by s.c. sutures.

Recombinant mouse IL-3 (100 ng/day in 10 μl injection volume) was injected intra-articularly in OA mice, whereas OA control mice received equal volume of PBS. Effect of IL-3 on OA-associated cartilage and subchondral bone degeneration was evaluated using four different treatment regimens, which were categorized into two different time points (days 15 and 43 postsurgery) and two different therapies (preventive and therapeutic). For day 15 studies, mice were injected with IL-3 from days 1 to 15 (as preventive therapy) and days 8 to 15 (as therapeutic therapy). For day 43 studies, mice were injected with IL-3 from days 1 to 43 (as preventive therapy) and days 8 to 43 (as therapeutic therapy). Mice were sacrificed on days 15 and 43, and limbs were preserved in 10% formalin. The microarchitecture of subchondral bone was evaluated by microcomputed tomography (μ-CT), and the changes in articular cartilage were assessed histologically.

Microcomputed tomography

μ-CT of excised bones was performed by a SkyScan 1076 CT scanner (SkyScan, Aartselaar, Belgium) as described previously (24, 25) and following the general guidelines for assessment of the bone microarchitecture in rodents using μ-CT (26). In brief, the knee joints of mice were scanned at 50 kV, 200 μA using a 0.5-mm aluminum filter and a resolution of 9 mm/pixel. Reconstruction of the sections was done by a modified Feldkamp cone-beam algorithm with beam hardening correction set to 50%. For morphometric quantification of subchondral bone, the region between articulating surface of condyles and growth plate in respective bones at knee joint was assessed. Various trabecular bone indices such as trabecular bone volume fraction (BV/TV; %), trabecular number (Tb. N.; 1/mm), connectivity density (Conn.D), structure model index (SMI), and trabecular pattern factor (Tb. Pf.; 1/mm) were evaluated using CT Analyzer software. The binary images of transaxial radiographs of subchondral bone microarchitecture for both femur and tibia were generated by Data Viewer software.

Histology

For histological analysis of mouse articular cartilage, formalin-fixed knee joints were decalcified, embedded in paraffin, and sectioned at a thickness of 5 μm. These sections were stained with H&E and structural integrity of cartilage was assessed microscopically. The histological sections were evaluated using OsteoArthritis Research Society International (OARSI) scoring system (27) with modifications: in brief, grade 0 = intact articulating surface and zones of cartilage, and appropriate orientation of chondrocytes; grade 1 = intact superficial zone, hypocellular cartilage, hypertrophic cells, and clonal clusters of chondrocytes near articulating surface; grade 2 = discontinuous articulating surface, degraded matrix, disoriented cells, clonal clusters with four cells, and hypertrophic chondrocytes in hypocellular cartilage; grade 3 = fissured cartilage along with degraded matrix and articulating surface, hypocellular cartilage with hypertrophic cells and clonal clusters with four to six chondrocytes; grade 4 = erosion of superficial zone and excavation of cartilage, clonal clusters with six to eight chondrocytes, hypocellular cartilage with hypertrophic cells and degraded matrix; grade 5 = denuded articulation, presence of fibrocartilage, cysts, and initiation of osteophyte formation; and grade 6 = deformations, osteophyte formation, bone remodeling, and fibrocartilaginous and osseous repair extending above the previous surface.

Statistical analysis

Results are represented as mean ± SEM. Statistical significance was calculated using one-way ANOVA with a subsequent post hoc Tukey's test for multiple comparisons. The significance values are defined as $^{*,\$,\#}p \le 0.05$, $^{**,\$\$,\#\#}p \le 0.01$, $^{***,\$\$\$,\#\#\#}p \le 0.001$, and $^{****,\$\$\$\$,\#\#\#\#}p \le 0.0001$.

Results

Mouse and human chondrocytes express IL-3R

To evaluate the effect of IL-3 on chondrocytes, we first examined the expression of IL-3Rα on both mouse and human chondrocytes. Primary cultures of both articular and sternal chondrocytes isolated from mouse knee balls and sternum, respectively, showed expression of Sox9 and IL-3Rα mRNA by RT-PCR (Fig. 1A). The protein expression of Sox9 and IL-3Rα on these chondrocytes was confirmed by Western blotting (Fig. 1B). We observed that in a homogenous population of chondrocytes, >90% of cells showed surface expression of IL-3Rα by flow cytometry (Fig. 1C). Fig. 1D represents the median fluorescence intensity showing expression of IL-3Rα and chondrocyte-specific molecules: aggrecan, Col2a and Sox9. The expression of IL-3Rα and chondrocyte-specific molecules was further confirmed by immunofluorescence microscopy (Fig. 1E). The gene expression of IL-3Rα was also confirmed on human cartilage tissues (Fig. 1F) and cultured human chondrocytes at passage 5 (Fig. 1G) along with the expression of chondrocyte-specific genes such as Sox9, Col2a, and aggrecan. The protein expression of IL-3Rα and Sox9 was also confirmed on human chondrocytes by Western blotting (Fig. 1H), and coexpression of IL-3Rα with Sox9 was observed by immunofluorescence microscopy (Fig. 1I). These results confirm that both mouse and human chondrocytes express IL-3Rα at gene and protein levels. The homogenous populations of mouse and human chondrocytes were used for all further studies.

Effect of IL-3 on proliferation and gene expression of chondrocytes

Because chondrocytes exhibited strong expression of IL-3Rα, we examined the effect of rIL-3 on proliferation and gene expression

Table I. Mouse and human primers used for RT-PCR and real-time PCRs

	Primer Sequences (5′–3′)		
Gene	Forward	Reverse	Amplicon Size (bp)
Mouse Sox9	CGG GGC TGG TAC TTG TAA TC	GAG CTC AGC AAG ACT CTG GG	131
Mouse Col2a	TGT CAT CGC AGA GGA CAT TC	CGG TCC TAC GGT GTC AGG	144
Mouse Aggrecan	CGC TCA GTG AGT TGT CAT GG	CTG AAG TTC TTG GAG GAG CG	134
Mouse IL-3Rα	CCT CTG ACC TCG ACT TGA CC	CTC CTT GGG TAC ACC CTG C	130
Mouse MMP-3	AGC CTT GGC TGA GTG GTA GA	TGG AGA TGC TCA CTT TGA CG	121
Mouse MMP-13	GGT CCT TGG AGT GAT CCA GA	CTG GAC CAA ACT ATG GTG GG	135
Mouse GAPDH	TTG AGG TCA ATG AAG GGG TC	TCG TCC CGT AGA CAA AAT GG	132
Human Sox9	GCC GAA AGC GGG CTC GAA AC	AAA AGT GGG GGC GCT TGC ACC	120
Human Col2a	CCT CCA GGT CTT CAG GGA AT	AGG AGG TCC AAC TTC TCC CT	195
Human Aggrecan	GCG AGT TGT CAT GGT CTG AA	TTC TTG GAG AAG GGA GTC CA	122
Human IL-3Rα	AGA CAC AGA CCA GGG CCA G	TAT GAA TTC TTG AGC GCC TG	130
Human MMP-1	GAG CTC AAC TTC CGG GTA GA	CCC AAA AGC GTG TGA CAG TA	121
Human MMP-3	AGC GTG AAT CTG TAT CTT GCC GGT	ACA GTC ACT TGT CTG TTG CAC ACG	142
Human MMP-13	TCA TGC TTT TCC TCC TGG GCC AAA	CGA ACT CAT GCG CAG CAA CAA GAA	116
Human β-actin	CTC CGT GTG GAT CGG CGG C	GAC GAT GGA GGG GCC GGA	100

of chondrocytes. Mouse (Fig. 2A, 2B) and human (Fig. 2C, 2D) chondrocytes were treated with varying concentrations of species-specific IL-3 for 72 h, and the proliferation of chondrocytes was analyzed by MTT assay (Fig. 2A, 2C). The dose-dependent effect of IL-3 on proliferation was also assessed after 72 h by BrdU incorporation ELISA (Fig. 2B, 2D). We observed that IL-3 does not affect the proliferation of both mouse and human chondrocytes, and showed no adverse effect on these cells. Further, we examined the effect of IL-3 on chondrocyte-specific gene expression by incubating mouse chondrocytes for 72 h with different concentrations of IL-3. IL-3 did not alter the expression of Sox9, Col2a, and aggrecan at all the concentrations. Also, IL-3 did not show any significant change in the expression of cartilage matrix-degrading enzymes, MMP-3 and MMP-13 (Fig. 2E). These results indicate that IL-3 does not alter the proliferation and gene expression of chondrocytes.

Next, we examined the effect of IL-3 on chondrogenic differentiation of human bone marrow–derived MSCs using micromass pellet culture assay. Human bone marrow MSCs (2×10^5 cells/well) were centrifuged in U-bottom 96-well plates, and micromass cell pellets were cultured for 21 d in chondrogenesis induction media with different concentrations of human IL-3. Histological sections of micromass pellets were assessed for the presence of chondrocytes, matrix deposition, and lacunae formation. MSCs differentiated into chondrocytes located in lacunae and showed matrix deposition. We observed no difference in chondrocyte differentiation, lacunae formation, and matrix deposition upon IL-3 treatment (Fig. 2F). Chondrogenic differentiation includes proteoglycan-rich matrix deposition, which was evaluated by staining with toluidine blue. IL-3–treated chondrogenic pellets showed matrix deposition similar to untreated chondrogenic con-

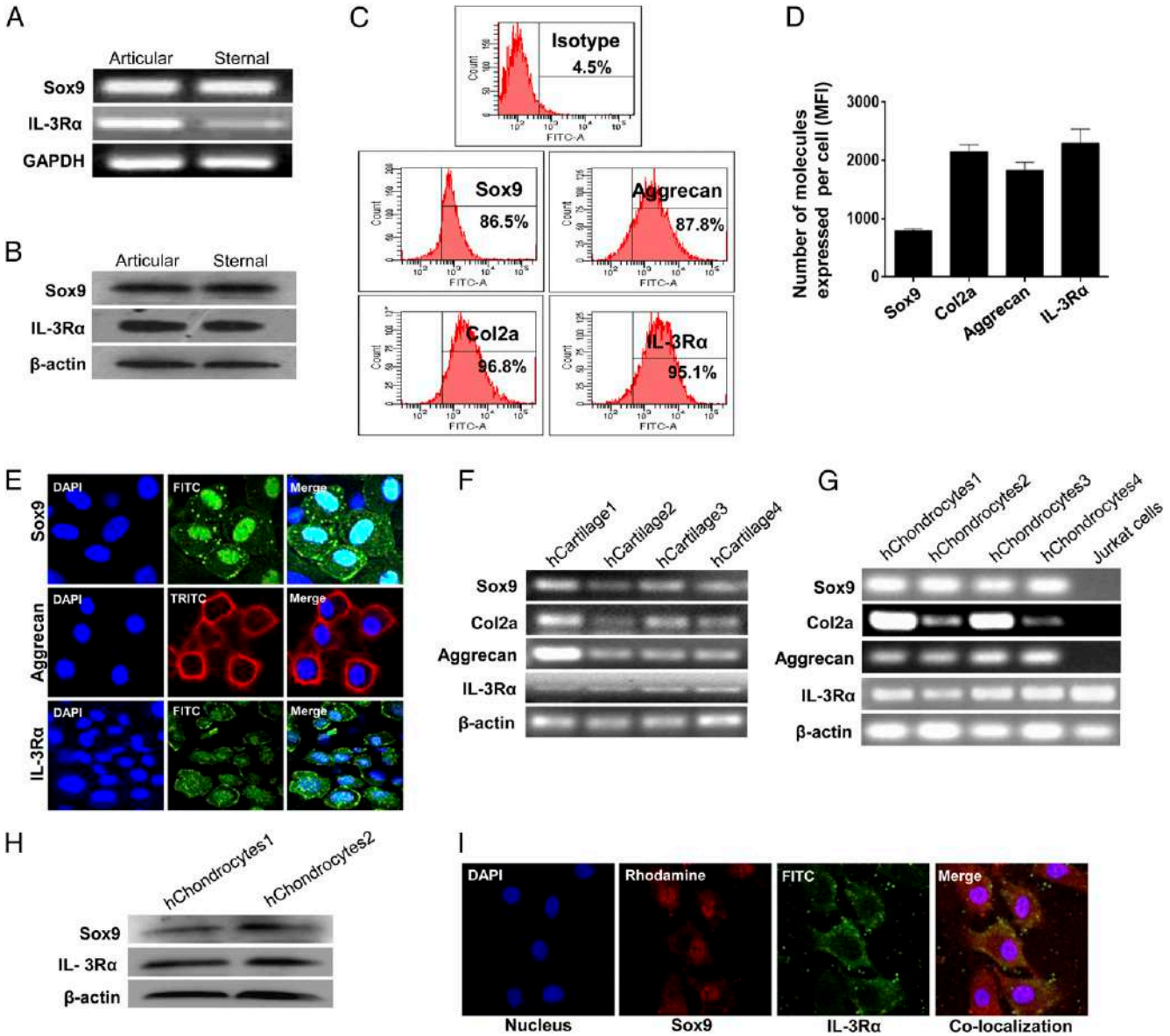

FIGURE 1. Expression of IL-3R on mouse and human chondrocytes. Presence of IL-3Rα and Sox9 on mouse chondrocytes was assessed by RT-PCR (**A**) and Western blotting (**B**). Percentage of chondrocytes exhibiting surface expression of IL-3Rα (**C**) and expression of IL-3Rα per cell represented as median fluorescence intensity (MFI) (**D**) were examined by flow cytometry. Bar graphs are expressed as mean ± SEM of three independent experiments. Surface expression of IL-3Rα on chondrocytes was confirmed by immunofluorescence microscopy (**E**). Human cartilage tissues (**F**) and cultured chondrocytes (**G**) were evaluated by RT-PCR for the expression IL-3Rα and chondrogenic markers. IL-3Rα expression on human chondrocytes was also assessed by Western blotting (**H**). Colocalization of Sox9 with IL-3Rα on human chondrocytes was examined by immunofluorescence microscopy. (**I**). Similar results were obtained in two or three independent experiments. Original magnification ×63.

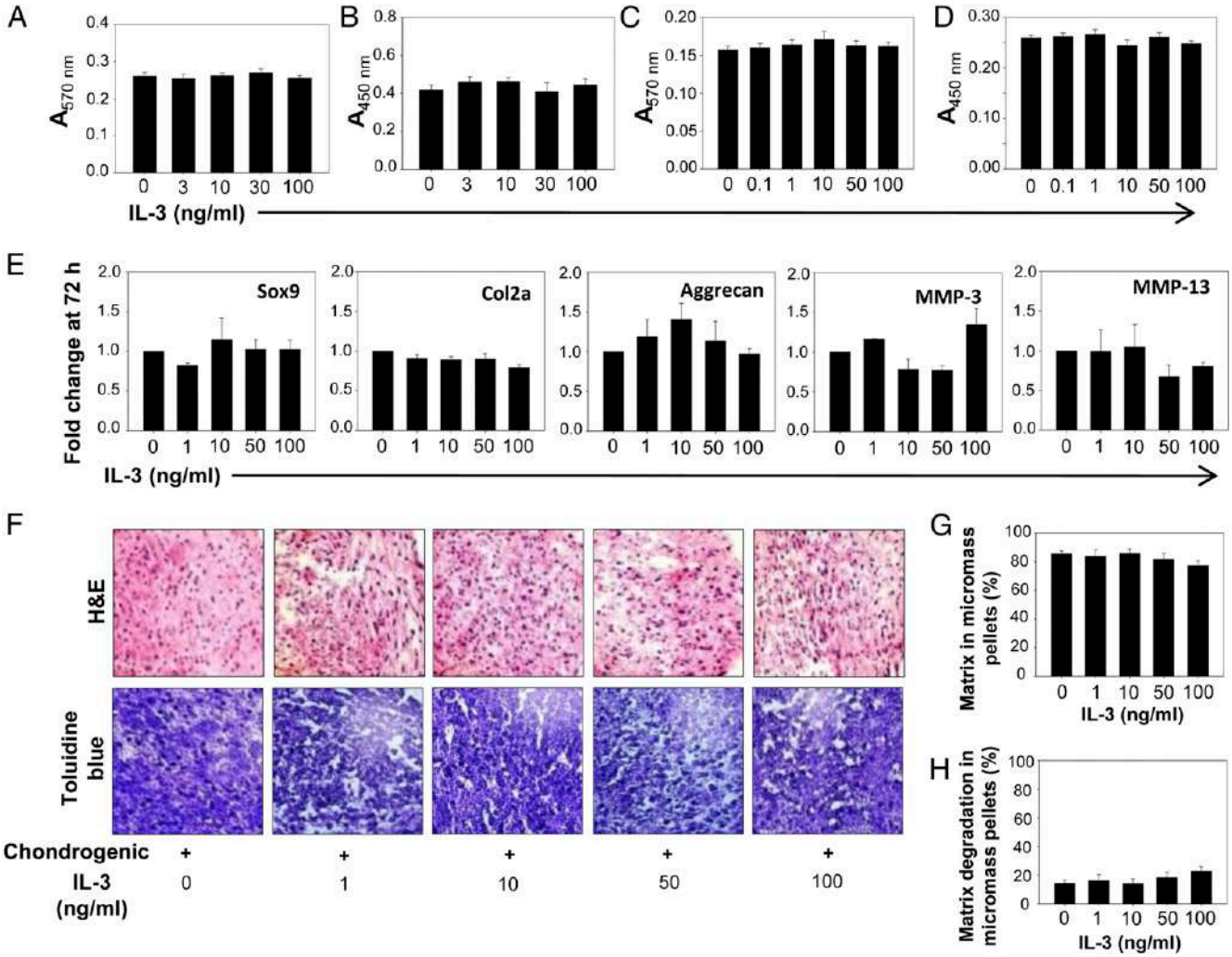

FIGURE 2. Effect of IL-3 on proliferation and differentiation of chondrocytes. Mouse (**A** and **B**) and human (**C** and **D**) chondrocytes (5×10^3 cells/well) were cultured in 96-well plates for 72 h with different concentrations of IL-3. Cell proliferation was assessed by MTT assay (A and C) and BrdU incorporation ELISA (B and D). Bar graphs are expressed as mean ± SEM of six replicates per group ($n = 6$). Similar results were obtained in four independent experiments. Effect of IL-3 on expression of Sox9, Col2a, aggrecan, MMP-3, and MMP-13 was examined by real-time PCR by incubating mouse chondrocytes for 72 h with or without different concentration of IL-3 (**E**). Results are average of three independent experiments. Human MSCs differentiated into chondrocytes in chondrogenesis induction medium in presence or absence of different concentrations of IL-3 were assessed for tissue histology and matrix deposition by H&E and toluidine blue staining, respectively. (**F**). The H&E-stained images were further quantitated for percent matrix (**G**) and percent matrix degradation (**H**) using ImageJ software. Similar results were obtained in two independent experiments. Original magnification ×40.

trols (Fig. 2F). Using image analysis software, we further quantitated the percent area covered by stained matrix and unstained white spaces in different regions of micromass pellet as a measure of matrix deposition and degradation, respectively. The percent matrix in IL-3–treated pellets was comparable with untreated chondrogenic pellets (Fig. 2G), and no degradation of matrix was observed upon IL-3 treatment (Fig. 2H). These data suggest that IL-3 does not change the functional properties of differentiating chondrocytes.

IL-3 reduces damage to cartilage matrix in vitro by downregulating proinflammatory cytokine–induced expression of MMPs

IL-1β and TNF-α are the key players in amplifying the inflammatory conditions and induces cartilage degeneration in OA joints (28, 29). Because IL-3 has an anti-inflammatory activity in vitro and in vivo (20, 21), we further investigated the effect of IL-3 on mouse chondrocytes in the presence of IL-1β. Mouse chondrocytes were incubated with IL-1β (5 ng/ml) and different concentrations of IL-3 for 24 h. IL-1β inhibited the expression of chondrocyte-specific genes including Sox9, Col2a, and aggrecan, and upregulated the expression of matrix-degrading enzymes, MMP-3 and MMP-13. In mouse chondrocytes, we observed that IL-3 significantly upregulated the expression of Sox9 and Col2a, which were downregulated by IL-1β. The expression of aggrecan was further downregulated in the presence of IL-3. Interestingly, IL-3 treatment significantly downregulated IL-1β–induced expression of matrix-degrading enzymes: MMP-3 at all the concentrations and MMP-13 at 50 and 100 ng/ml IL-3 (Fig. 3A). This suggests an anabolic role of IL-3 on cartilage matrix by promoting synthesis of matrix components and by downregulation of matrix-degrading enzymes secreted by chondrocytes. In human chondrocytes, both IL-1β and TNF-α individually, as well as in combination, downregulated the expression of Col2a and aggrecan, which was not restored upon IL-3 treatment. No change in the expression of Sox9 was observed in all the groups. IL-3 downregulated the expression of MMP-1, MMP-3, and MMP-13 induced by IL-1β or TNF-α alone. Interestingly, the synergistic effect of IL-1β and TNF-α on the increased expression of all these MMPs was downregulated by IL-3 (Fig. 3B). These data suggest the role of IL-3 in reducing the catabolic processes induced in chondrocytes by

proinflammatory cytokines. It also suggests that under inflammatory conditions, IL-3 reduces cartilage damage by regulating matrix degradation mediated by MMPs along with neomatrix synthesis.

IL-3 reduces cartilage degeneration in mouse model of human OA

In joint articulation, articular cartilage is the prime tissue involved in OA. Because IL-3 prevented cartilage degeneration in vitro, we assessed the in vivo role of IL-3 on OA-associated cartilage damage. For this, we developed an OA model in C57BL/6 mice by surgical transection of ACL. Cartilage in knee joints was evaluated histologically for OA changes at day 8 after ACL transection. The H&E-stained sections of knee joints in OA mice showed disrupted and discontinuous (blue arrows) cartilage, hypocellular cartilage with clonal clusters (black arrows), and presence of hypertrophic chondrocytes or empty lacunae (red arrows) toward the articulating

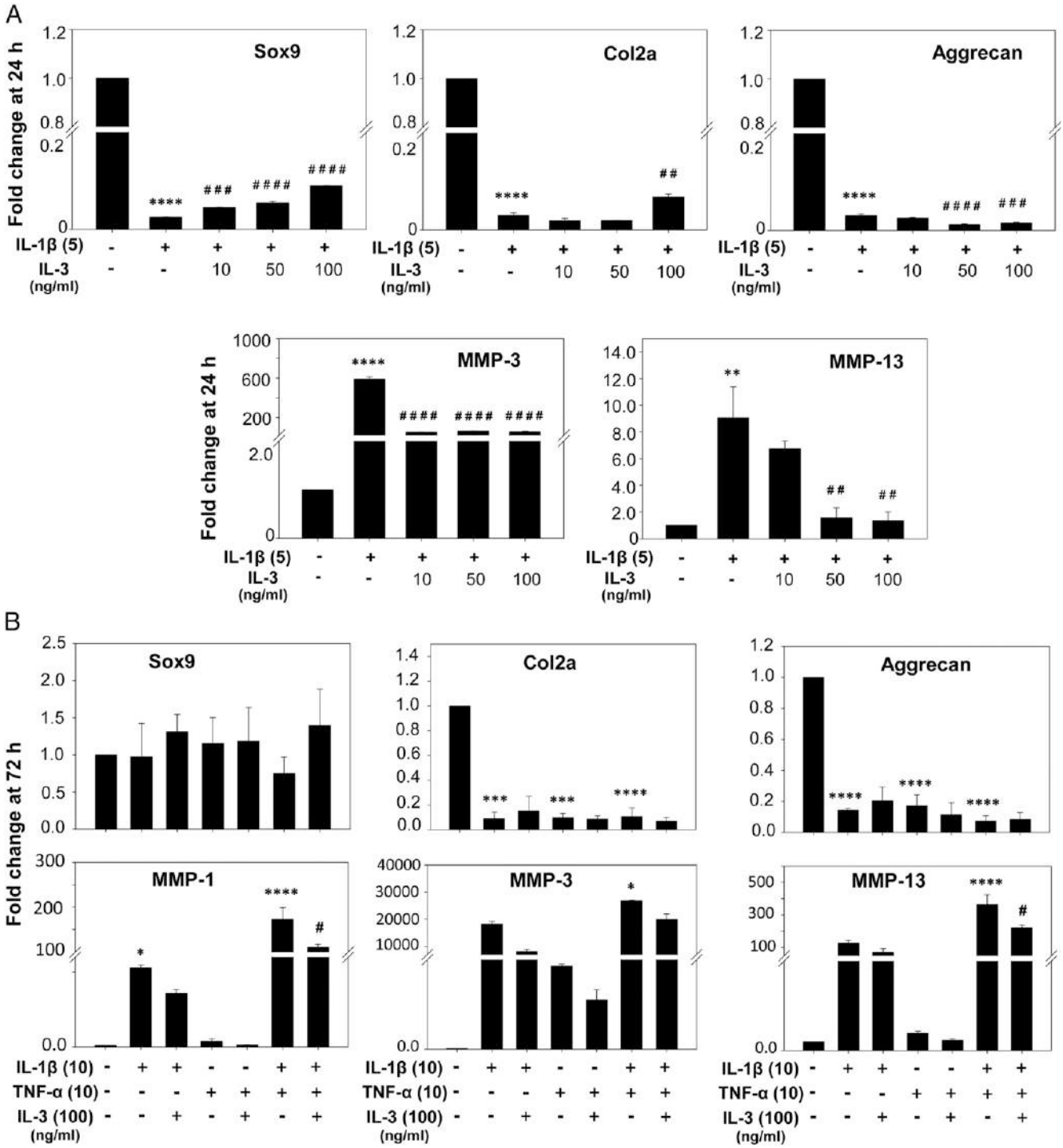

FIGURE 3. IL-3 downregulates proinflammatory cytokine-induced expression of matrix-degrading enzymes. Mouse (**A**) and human (**B**) chondrocytes were treated with IL-1β and/or TNF-α and different concentrations of IL-3 for 24 and 72 h, respectively. The expression of chondrocyte-specific genes and matrix-degrading enzymes, MMP-1, MMP-3, and MMP-13, was evaluated by real-time PCR. Significance was calculated by a one-way ANOVA with a post hoc Tukey's multiple comparisons test. Results are the average of three (A) and four (B) independent experiments. $^{*}p < 0.05$, $^{**}p < 0.01$, $^{***}p < 0.001$, $^{****}p < 0.0001$ versus untreated controls; $^{\#}p < 0.05$, $^{\#\#}p < 0.01$, $^{\#\#\#}p < 0.001$, $^{\#\#\#\#}p < 0.0001$ versus IL-1β– and/or TNF-α–treated groups.

surface (Supplemental Fig. 1A). The superficial zone of resting cells was either eroded or differentiated to hypertrophic stage. Further, evaluation of these histological sections using a modified OARSI scoring system showed a significant degeneration of articular cartilage in OA mice (Supplemental Fig. 1B). These observations confirmed the degeneration of cartilage associated with OA, as well as the development of mouse model of human OA within 8 d of ACL transection.

Next, the effect of mouse IL-3 (100 ng/day by intra-articular injection) on cartilage degeneration was evaluated using four different treatment regimens, which were categorized into two different time points (days 15 and 43 postsurgery) and two different therapies (preventive and therapeutic). For day 15 studies, mice were injected with IL-3 from days 1 to 15 (as preventive therapy) and days 8 to 15 (as therapeutic therapy). For day 43 studies, mice were injected with IL-3 from days 1 to 43 (as preventive therapy) and days 8 to 43 (as therapeutic therapy). Mice were sacrificed on days 15 and 43. In H&E-stained sections of knee joints, we observed degeneration of articular cartilage in OA mice. As compared to disrupted and discontinuous cartilage (blue arrows) in OA mice, there was distinct cartilage articulation and reduced number of hypertrophic chondrocytes in different zones of cartilage in all groups of OA mice treated with IL-3. Also, there were reduced numbers of clonal clusters (black arrows) and hypertrophic cells (red arrows) near the articulating surface of cartilage in IL-3–treated OA mice (Fig. 4A). Further, OARSI-based histological evaluation of knee joint sections showed a significant degeneration of articular cartilage in OA mice. Interestingly, reduced disease severity was observed in all OA mice treated with IL-3 at days 15 and 43 in both preventive and therapeutic regimens as represented in box-and-whisker plot for histological score (Fig. 4B).

Because IL-3 decreased the in vitro expression of MMPs in both mouse and human chondrocytes induced by proinflammatory cytokines, we further checked the effect of IL-3 on these MMPs in vivo in OA mice. Tissue lysates from knee joints of sham, OA, and IL-3–treated OA mice were examined for the presence of MMPs by Western blotting. We found that IL-3 decreased the OA-induced expression of MMP-3 and MMP-13 at day 15 in both preventive and therapeutic treatment regimens (Fig. 4C). However, at day 43, IL-3 decreased these MMPs only in the preventive treatment regimen (Fig. 4D). IL-3 also showed decreased trend, although nonsignificant, in total MMP-3 levels in some treatment regimens as examined by ELISA (Supplemental Fig. 2). All these results suggest that IL-3 plays an important role in reducing cartilage degeneration by regulating the expression of MMPs in OA conditions.

IL-3 decreases degeneration of trabecular microarchitecture of subchondral bone in OA mice

Articular cartilage and subchondral bone constitute the important components of joint articulation. In OA, the degenerative changes in articular cartilage gradually percolate into the subchondral region as both are interdependent (30). ACL transection alters the joint biomechanics and subsequently leads to the development of OA (23). In our mouse model of human OA, the binary images of transaxial radiographs generated by μ-CT of femoral subchondral bone showed destruction of trabecular microarchitecture within 8 d of ACL transection (Supplemental Fig. 3A). In the femoral subchondral bone, trabecular bone volume, connectivity, and geometry of connection were determined. In ACL transected mice, trabecular BV/TV was lower and SMI and Tb. Pf. were higher than the sham control, indicating reduced bone volume and poor geometry (Supplemental Fig. 3B). Topological parameters including Tb. N. and Conn.D were also determined to evaluate the connectivity of subchondral bone. Both Tb. N. and Conn.D are inversely related to Tb. Pf. (26). We observed a significant decrease in Tb. N. and Conn.D, and an increase in Tb. Pf. in OA mice compared with sham controls (Supplemental Fig. 3B). These data suggest the erosion of trabecular bone in the femoral subchondral region and confirmed the development of OA within 8 d of ACL transection in mice. However, no OA-associated changes were observed in tibial subchondral bone (Supplemental Fig. 3C, 3D).

Next, the subchondral bone of IL-3–treated OA mice was evaluated using four different treatment regimens as described earlier. The representative images of trabecular microarchitecture of femoral subchondral bone showed betterment upon IL-3 treatment in both preventive and therapeutic regimens at day 15 (Fig. 5A). The trabecular microarchitecture in IL-3–treated OA mice showed a significant increase in Conn.D in therapeutic treatment regimen and a trend toward improvement in SMI and Tb. Pf. in both preventive and therapeutic treatment regimens. However, no effect on BV/TV and Tb. N. was seen in IL-3–treated mice (Fig. 5B). At day 43, the representative images of trabecular microarchitecture of femoral subchondral bone also showed betterment upon IL-3 treatment in both preventive and therapeutic treatment regimens (Fig. 5C). IL-3 showed significant preservation of SMI and Conn.D in both treatment regimens, whereas Tb. Pf. was significantly protected in the therapeutic treatment regimen. A trend of improvement in BV/TV and Tb. N. was observed in both treatment regimens (Fig. 5D). Tibial subchondral bone showed milder symptoms of OA, and the effect of IL-3 was not evident in OA mice (Supplemental Fig. 4). These results suggest that IL-3 plays an important role in preserving femoral subchondral bone microarchitecture in OA stress.

IL-3 reduces IL-1β–induced matrix degradation in pellet cultures of human MSCs

Because IL-3 reduces cartilage degeneration in OA mice, we determined the effect of IL-3 on matrix secreted during human chondrocyte differentiation in the presence of IL-1β. We first examined the preventative effect of IL-3 on matrix degradation by treating micromass pellets of human MSCs with IL-1β (5 ng/ml) and two concentrations of IL-3 (50 and 100 ng/ml) from days 1 to 21 (Fig. 6A). Histological evaluation showed that the matrix in IL-3–treated chondrogenic pellets was less degraded compared with IL-1β, as indicated by reduced white spaces and increased matrix (pink) in H&E-stained sections (Fig. 6B). Quantitation of percent matrix deposition (Fig. 6C) and percent matrix degradation (Fig. 6D) by image analysis confirmed that IL-3 (100 ng/ml) significantly reduces the matrix degradation induced by IL-1β.

Therapeutic effects of IL-3 on IL-1β–induced matrix degradation in human MSCs

Next, we wanted to determine whether IL-3 could also help in repairing IL-1β–induced matrix degradation. For this, the cell pellets were primed with IL-1β (5 ng/ml) for the first 10 d, and IL-3 (50 ng/ml) was added from days 10 to 21 (Fig. 7A). Histological analysis showed that IL-3 reduced matrix degradation induced by IL-1β (Fig. 7B), increased percent matrix (Fig. 7C), and decreased percent degradation of matrix (Fig. 7D). These results suggest that IL-3 shows a protective effect when the process of matrix degradation was initiated by IL-1β. Further, we examined the therapeutic effect of IL-3 on IL-1β–induced matrix degradation by incubating cell pellets with IL-1β from days 1 to 21, and IL-3 (50 and 100 ng/ml) was added from days 10 to 21 (Fig. 7E). Interestingly, we observed that IL-3 showed therapeutic effect and decreases further degradation of matrix under severe inflammatory conditions (Fig. 7F) as indicated by increased percent matrix

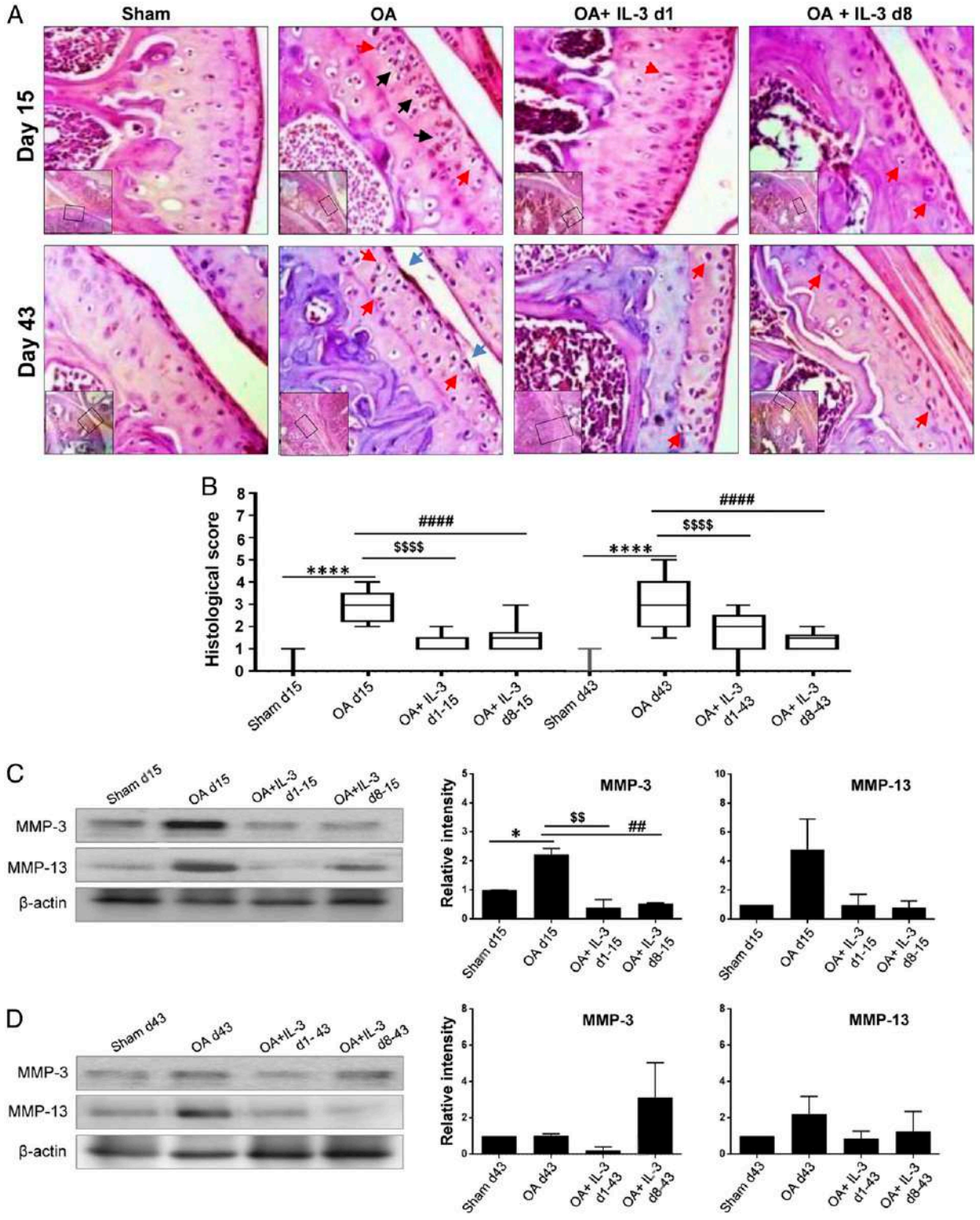

FIGURE 4. IL-3 reduces OA-associated degeneration of cartilage in mouse model of human OA. ACL-transected mice were injected intra-articularly with IL-3 (100 ng/day) using four different treatment regimens, which were categorized into two different time points (days 15 and 43 postsurgery) and two different therapies (preventive and therapeutic). For day 15 studies, mice were injected with IL-3 from days 1 to 15 (as preventive therapy) and days 8 to 15 (as therapeutic therapy). For day 43 studies, mice were injected with IL-3 from days 1 to 43 (as preventive therapy) and days 8 to 43 (as therapeutic therapy). Mice were sacrificed on days 15 and 43. H&E-stained knee joint sections were evaluated for damage to cartilage articulation (blue arrows), zonation and cell phenotype (red arrows), and clonal clusters of chondrocytes (black arrows) (**A**). Original magnification ×40. The OARSI score based histological assessment of articular cartilage in various experimental groups is represented as box-and-whisker plot (**B**). Data are pooled from three independent experiments with 10–14 mice/group. Expression of total MMP-3 and MMP-13 at days 15 (**C**) and 43 (**D**) was examined by Western blotting, and relative intensities were calculated by densitometry using ImageJ software. Bar graphs are expressed as mean ± SEM of two independent experiments. Significance was calculated by a one-way ANOVA with a post hoc Tukey's multiple comparisons test between 1) OA versus sham, 2) OA+IL-3d1 groups (where IL-3 treatment started from day 1) versus OA, and 3) OA + IL-3d8 groups (where IL-3 treatment started from day 8) versus OA. $^{*}p < 0.05$ or $^{****}p < 0.0001$ for OA versus sham; $^{\$\$}p < 0.01$ or $^{\$\$\$\$}p < 0.0001$ for OA+IL-3d1 versus OA; $^{\#\#}p < 0.01$ or $^{\#\#\#\#}p < 0.0001$ for OA+IL-3d8 versus OA.

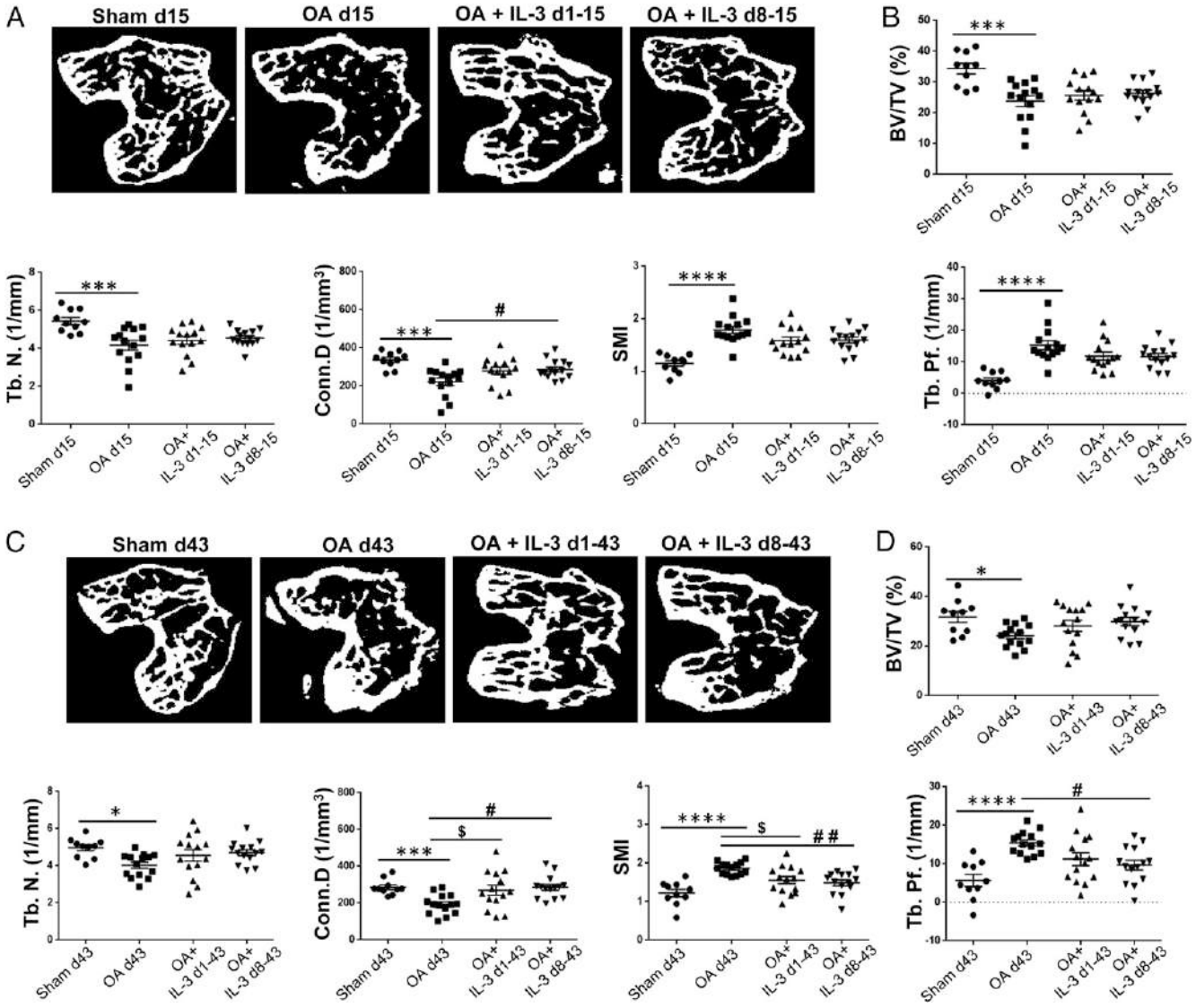

FIGURE 5. IL-3 reduces degradation of subchondral bone in OA mice. ACL-transected mice were injected intra-articularly with IL-3 (100 ng/day) using four different treatment regimens as described in Fig. 4. Whole knee joints were subjected to μ-CT for evaluation of subchondral bone. Representative binary radiographs show the trabecular bone structure of various experimental groups at days 15 (**A**) and 43 (**C**). Various trabecular bone indices reflecting the quality of subchondral bone and topological parameters including BV/TV, Tb. N., Conn.D, SMI, and Tb. Pf. (**B** and **D**) were quantified at days 15 (B) and 43 (D) using μ-CT reconstructions. Data are pooled from three independent experiments and are presented as mean ± SEM of 10–14 mice/group. Significance was calculated by a one-way ANOVA with a post hoc Tukey's multiple comparisons test between: 1) OA versus sham, 2) OA+IL-3d1 groups versus OA, and 3) OA+IL-3d8 groups versus OA. $^{*}p < 0.05$, $^{***}p < 0.001$, or $^{****}p < 0.0001$ for OA versus sham; $^{\$}p < 0.05$ for OA+IL-3d1 versus OA; $^{\#}p < 0.05$ or $^{\#\#}p < 0.01$ for OA+IL-3d8 versus OA.

(Fig. 7G) and decreased percent degradation (Fig. 7H). These results support that the downregulation of MMPs by IL-3 at transcript level is reducing the degradation of cartilage matrix in inflammatory conditions induced by OA stress.

Discussion

Chondrocytes participate in anabolic-catabolic balance required for maintenance of cartilage by modulating synthesis and degradation of its matrix (31). Chondrocytes lose their proliferative potential upon terminal differentiation, rendering them incapable to compensate for the cartilage damage (11, 12). Also, any pathological stress that disturbs this anabolic-catabolic balance subsequently induces inflammation and alters the balance of anti-inflammatory and proinflammatory cytokines in the joint microenvironment (9). This aggravates the degenerative process, resulting in irreversible physical damage to cartilage, and gradually involves the whole joint with increase in the severity of OA (29). Besides this, inflammation attracts immune cells and osteoclast precursors, thereby increasing osteoclast formation and bone resorption in subchondral region (32). Various studies have shown that proinflammatory cytokines affect survival and phenotype of chondrocytes in several ways. These cytokines downregulate the expression of genes involved in maintenance of cartilage matrix, and promote hypertrophy and apoptosis of chondrocytes (14). In addition, they induce expression of MMPs, which degrade cartilage matrix, thereby aggravating the degeneration of joints (15). We have previously shown that IL-3 is a potent inhibitor of osteoclast formation and pathological bone resorption in vitro (17–20), and it protects cartilage and bone damage in murine models of inflammatory arthritis (20) and collagen-induced arthritis (21). In this study, we investigated the role of IL-3 in regulation of chondrocyte function in vitro and cartilage degradation in vivo in a mouse model of human OA.

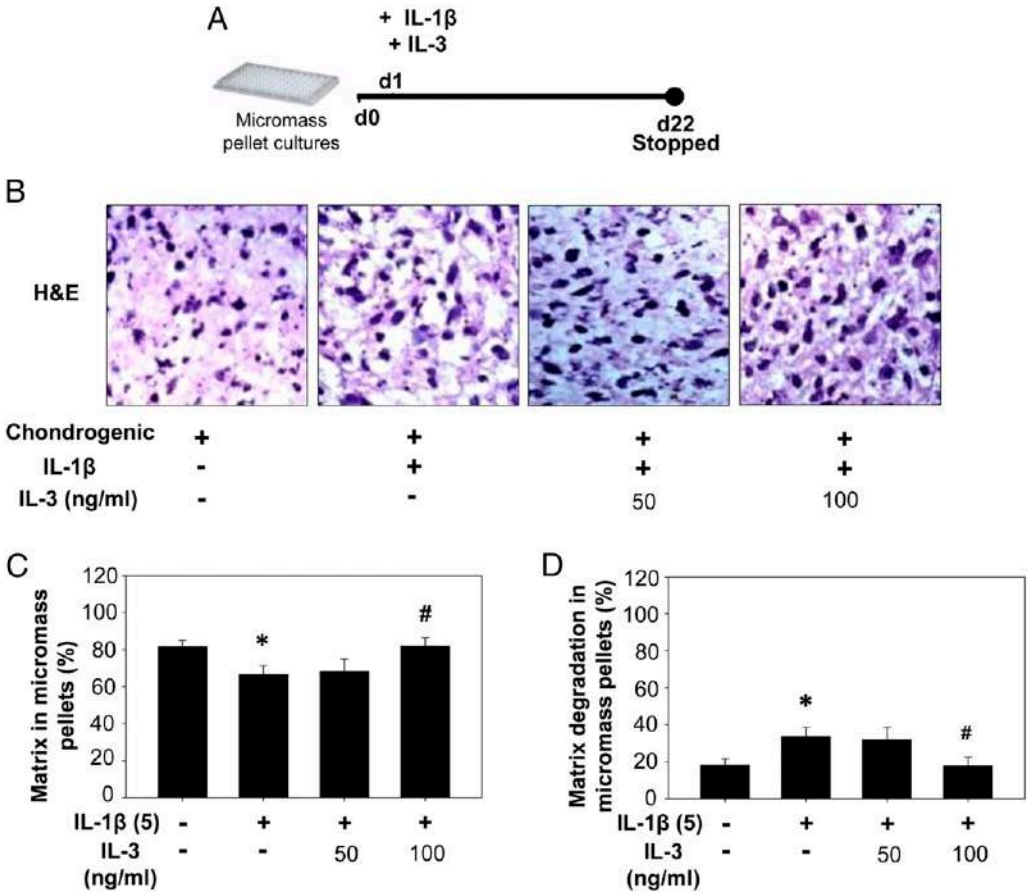

FIGURE 6. Preventive effect of IL-3 on IL-1β–induced matrix damage in chondrogenic micromass pellets of human MSCs. Human MSCs (2×10^5 cells) were cultured as micromass pellets in chondrogenesis induction medium in the presence of IL-1β (5 ng/ml) and IL-3 (50 and 100 ng/ml) from days 1 to 21 (**A**). Chondrogenic pellets were evaluated for histology and matrix deposition (**B**). Original magnification ×40. The percent matrix (**C**) and percent matrix degradation (**D**) were assessed from H&E-stained sections using ImageJ software. Bar graphs represent mean ± SEM. Similar results were obtained in three independent experiments. $^{*}p < 0.05$ for IL-1β versus untreated controls, $^{\#}p < 0.05$ for IL-3 versus IL-1β.

We first confirmed that chondrocytes are responsive to IL-3 by checking the expression of IL-3Rα on both mouse and human chondrocytes. The high affinity receptor for IL-3 consists of a heterodimer of IL-3–specific α-chain and a common β-chain, which is shared with GM-CSF and IL-5 (33). IL-3Rα is expressed by human hematopoietic stem cells (34), endothelial cells and monocytes (35), activated T cells (21), osteoclasts (17–19), osteoblasts, and MSCs (36). In this study, we report for the first time, to our knowledge, that both mouse and human chondrocytes express IL-3Rα at transcript and protein levels. When the effect of IL-3 was examined on the maintenance of cartilage by chondrocytes, we observed that IL-3 does not alter chondrocyte proliferation, gene expression, and matrix maintenance under nonpathological conditions. Interestingly, IL-3 significantly upregulated the expression of genes important for the synthesis of cartilage matrix such as Sox9 and Col2a in mouse chondrocytes, which were downregulated by IL-1β. Moreover, IL-3 significantly downregulated IL-1β–induced expression of matrix-degrading enzymes, MMP-3 and MMP-13. Interestingly, IL-3 downregulated the expression of matrix-degrading enzymes, MMP-1, MMP-3, and MMP-13, in human chondrocytes in the presence of proinflammatory cytokines, whereas no change in the expression of Sox9, Col2a, and aggrecan was observed. This suggests that IL-3 exerts its protective action by downregulating the expression of matrix-degrading enzymes induced by proinflammatory cytokines and also promotes neomatrix synthesis without increasing the proliferative potential of mouse chondrocytes. Whereas in humans, IL-3 mainly acts by downregulating matrix-degrading enzymes induced in the presence of proinflammatory cytokines. The components of cartilage matrix, collagens and proteoglycans, constitute the substrate for these MMPs. MMP-13, also known as collagenase-3, mainly degrades Col2a and, therefore, plays a central role in the progression of cartilage degeneration. Compared with other MMPs, MMP-13 has a higher catalytic activity for Col2a and gelatin, thereby making it the most potent peptidolytic enzyme among collagenase family (37). Also, MMP-13 overexpressing transgenic mice undergo spontaneous degeneration of articular cartilage characterized by excessive degradation of Col2a and aggrecan loss (38). We observed that IL-3 reduces cartilage damage mainly by downregulating the expression of MMPs and subsequent matrix degradation, as well as by promoting neomatrix synthesis in some cases and not by enhancing the proliferative potential of chondrocytes. To assess the translational implication of this observation, IL-1β–treated micromass pellets of human MSCs were cultured in the presence of IL-3 during the course of chondrogenic differentiation and were evaluated for matrix degradation. In agreement with other reports, we also observed that IL-1β hampers matrix deposition and induces its degradation (39, 40). Interestingly, IL-3 showed both preventive and therapeutic effect on IL-1β–induced matrix degradation. These observations supported that the decreased matrix degradation by IL-3 is a result of transcriptional downregulation of MMPs.

We further validated our in vitro studies by examining the in vivo effect of IL-3 in a mouse model of human OA. The present scientific understanding of OA suggests that the degeneration in cartilage

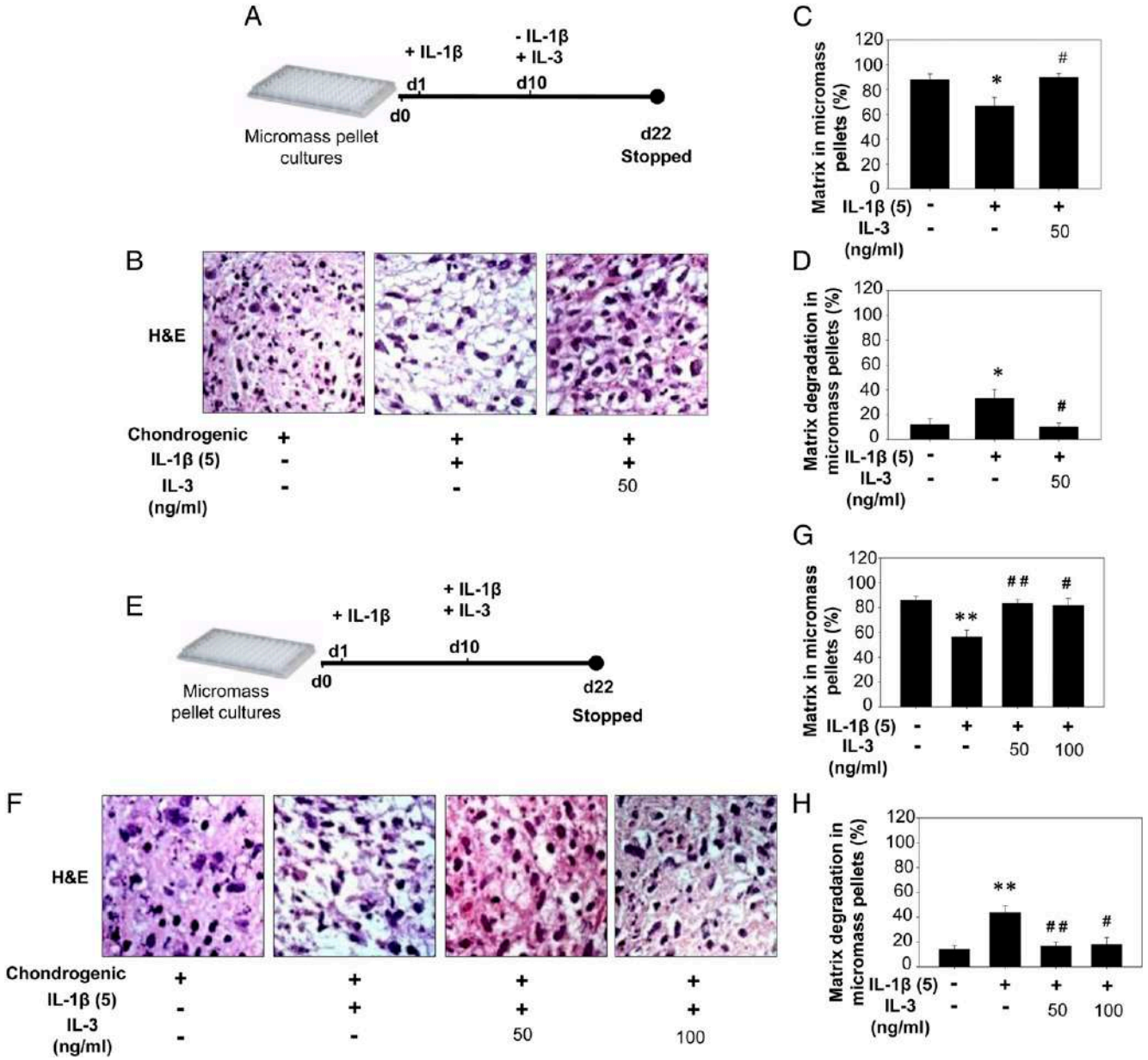

FIGURE 7. Therapeutic effect of IL-3 on IL-1β–induced matrix damage in chondrogenic micromass pellets of human MSCs. Human MSCs (2×10^5 cells) were cultured as micromass pellets in chondrogenesis induction medium in the presence of IL-1β (5 ng/ml) for 10 or 21 d, and IL-3 (50 or 100 ng/ml) was added from days 10 to 21 (**A** and **E**). Chondrogenic pellets were evaluated for pellet histology and matrix deposition (**B** and **F**). Original magnification ×40. The percent matrix (**C** and **G**) and percent matrix degradation (**D** and **H**) were assessed from H&E-stained sections using ImageJ software. Bar graphs represent mean ± SEM. Similar results were obtained in three independent experiments. $^{*}p < 0.05$ or $^{**}p < 0.01$ for IL-1β versus untreated controls; $^{\#}p < 0.05$ or $^{\#\#}p < 0.001$ for IL-3 versus IL-1β.

parallels microarchitectural changes in subchondral bone (41). We evaluated both articular cartilage and subchondral bone in an ACL-transected mouse model to understand the role of IL-3 in the pathophysiology of OA. Microscopic evaluation showed hypertrophic chondrocytes toward the articulating surface of cartilage within 8 d of ACL transection. This suggests that the inflammatory conditions developed because of altered biomechanical stress in ACL-transected joints advances chondrocytes toward terminal differentiation. This process lays a foundation for osteophyte formation in OA joints as well as cartilage thinning by expansion of subchondral bone into cartilage (42, 43). In IL-3–injected OA mice, a proper cartilage zonation reflecting the structural integrity of cartilage was maintained along with the maintenance of zone-specific phenotype of chondrocytes. Also, the reduced number of clonal clusters in articular cartilage upon IL-3 treatment suggests the decreased severity of disease progression. This was confirmed by the decreased levels of OA-induced MMP-3 and MMP-13 in IL-3–treated OA joints.

Articular cartilage and subchondral bone are interdependent entities, and the tissue origin of OA is uncertain (3, 4). ACL transection alters biomechanics of the joint that attracts inflammatory mediators and osteoclast precursors in the affected joints. The newly formed osteoclasts from these precursors along with resident osteoclasts promote subchondral bone resorption. OA-associated damage reaches its peak in 15 d and remains persistent thereafter (23). Evaluation of subchondral bone in OA mice showed significant damage to trabecular microarchitecture within 8 d of ACL transection and was observed until day 43. The quality

and trabecular microarchitecture of femoral subchondral bone was improved upon IL-3 treatment in OA mice at day 43. The protection of subchondral bone in the presence of IL-3 could be attributed to decreased osteoclast formation, and hence the bone resorption in the subchondral region (17–19). However, tibial subchondral bone showed milder symptoms of OA, and the protective effect of IL-3 was not evident. The in vitro and in vivo studies in mice strongly suggest that IL-3 has a multifaceted role in amelioration of cartilage and subchondral bone damage in addition to modulating the inflammatory response associated with OA. We also speculate that the downregulation of MMPs by IL-3 might be responsible for protection of cartilage in earlier models of arthritis (20, 21) by reducing the availability of cartilage-derived Ags in the joint microenvironment, leading to diminution of inflammatory conditions. Thus, our results suggest that IL-3 has a therapeutic potential for cartilage and bone degeneration associated with OA.

Acknowledgments

We thank Drs. Amod Kale and Pralhad Wangikar for histopathological assessment.

Disclosures

The authors have no financial conflicts of interest.

References

1. Blagojevic, M., C. Jinks, A. Jeffery, and K. P. Jordan. 2010. Risk factors for onset of osteoarthritis of the knee in older adults: a systematic review and meta-analysis. *Osteoarthritis Cartilage* 18: 24–33.
2. Felson, D. T. 2013. Osteoarthritis as a disease of mechanics. *Osteoarthritis Cartilage* 21: 10–15.
3. Baker-LePain, J. C., and N. E. Lane. 2012. Role of bone architecture and anatomy in osteoarthritis. *Bone* 51: 197–203.
4. Cox, L. G., C. C. van Donkelaar, B. van Rietbergen, P. J. Emans, and K. Ito. 2013. Alterations to the subchondral bone architecture during osteoarthritis: bone adaptation vs endochondral bone formation. *Osteoarthritis Cartilage* 21: 331–338.
5. Goldring, S. R., and M. B. Goldring. 2010. Bone and cartilage in osteoarthritis: is what's best for one good or bad for the other? *Arthritis Res. Ther.* 12: 143.
6. Chen, A. C., M. M. Temple, D. M. Ng, N. Verzijl, J. DeGroot, J. M. TeKoppele, and R. L. Sah. 2002. Induction of advanced glycation end products and alterations of the tensile properties of articular cartilage. *Arthritis Rheum.* 46: 3212–3217.
7. Erlebacher, A., E. H. Filvaroff, S. E. Gitelman, and R. Derynck. 1995. Toward a molecular understanding of skeletal development. *Cell* 80: 371–378.
8. Mackie, E. J., L. Tatarczuch, and M. Mirams. 2011. The skeleton: a multi-functional complex organ: the growth plate chondrocyte and endochondral ossification. *J. Endocrinol.* 211: 109–121.
9. Homandberg, G. A., F. Hui, C. Wen, C. Purple, K. Bewsey, H. Koepp, K. Huch, and A. Harris. 1997. Fibronectin-fragment-induced cartilage chondrolysis is associated with release of catabolic cytokines. *Biochem. J.* 321: 751–757.
10. Liu-Bryan, R., and R. Terkeltaub. 2015. Emerging regulators of the inflammatory process in osteoarthritis. *Nat. Rev. Rheumatol.* 11: 35–44.
11. van der Kraan, P. M. 2012. Osteoarthritis year 2012 in review: biology. *Osteoarthritis Cartilage* 20: 1447–1450.
12. Dreier, R. 2010. Hypertrophic differentiation of chondrocytes in osteoarthritis: the developmental aspect of degenerative joint disorders. *Arthritis Res. Ther.* 12: 216.
13. Pettipher, E. R., G. A. Higgs, and B. Henderson. 1986. Interleukin 1 induces leukocyte infiltration and cartilage proteoglycan degradation in the synovial joint. *Proc. Natl. Acad. Sci. USA* 83: 8749–8753.
14. Kobayashi, M., G. R. Squires, A. Mousa, M. Tanzer, D. J. Zukor, J. Antoniou, U. Feige, and A. R. Poole. 2005. Role of interleukin-1 and tumor necrosis factor alpha in matrix degradation of human osteoarthritic cartilage. *Arthritis Rheum.* 52: 128–135.
15. Loeser, R. F. 2006. Molecular mechanisms of cartilage destruction: mechanics, inflammatory mediators, and aging collide. *Arthritis Rheum.* 54: 1357–1360.
16. Tetlow, L. C., D. J. Adlam, and D. E. Woolley. 2001. Matrix metalloproteinase and proinflammatory cytokine production by chondrocytes of human osteoarthritic cartilage: associations with degenerative changes. *Arthritis Rheum.* 44: 585–594.
17. Khapli, S. M., L. S. Mangashetti, S. D. Yogesha, and M. R. Wani. 2003. IL-3 acts directly on osteoclast precursors and irreversibly inhibits receptor activator of NF-kappa B ligand-induced osteoclast differentiation by diverting the cells to macrophage lineage. *J. Immunol.* 171: 142–151.
18. Yogesha, S. D., S. M. Khapli, and M. R. Wani. 2005. Interleukin-3 and granulocyte-macrophage colony-stimulating factor inhibits tumor necrosis factor (TNF)-alpha-induced osteoclast differentiation by down-regulation of expression of TNF receptors 1 and 2. *J. Biol. Chem.* 280: 11759–11769.
19. Gupta, N., A. P. Barhanpurkar, G. B. Tomar, R. K. Srivastava, S. Kour, S. T. Pote, G. C. Mishra, and M. R. Wani. 2010. IL-3 inhibits human osteoclastogenesis and bone resorption through downregulation of c-Fms and diverts the cells to dendritic cell lineage. *J. Immunol.* 185: 2261–2272.
20. Yogesha, S. D., S. M. Khapli, R. K. Srivastava, L. S. Mangashetti, S. T. Pote, G. C. Mishra, and M. R. Wani. 2009. IL-3 inhibits TNF-alpha-induced bone resorption and prevents inflammatory arthritis. *J. Immunol.* 182: 361–370.
21. Srivastava, R. K., G. B. Tomar, A. P. Barhanpurkar, N. Gupta, S. T. Pote, G. C. Mishra, and M. R. Wani. 2011. IL-3 attenuates collagen-induced arthritis by modulating the development of Foxp3+ regulatory T cells. *J. Immunol.* 186: 2262–2272.
22. Pittenger, M. F., A. M. Mackay, S. C. Beck, R. K. Jaiswal, R. Douglas, J. D. Mosca, M. A. Moorman, D. W. Simonetti, S. Craig, and D. R. Marshak. 1999. Multilineage potential of adult human mesenchymal stem cells. *Science* 284: 143–147.
23. Zhen, G., C. Wen, X. Jia, Y. Li, J. L. Crane, S. C. Mears, F. B. Askin, F. J. Frassica, W. Chang, J. Yao, et al. 2013. Inhibition of TGF-β signaling in mesenchymal stem cells of subchondral bone attenuates osteoarthritis. *Nat. Med.* 19: 704–712.
24. Khan, M. P., A. K. Singh, A. A. Joharapurkar, M. Yadav, S. Shree, H. Kumar, A. Gurjar, J. S. Mishra, M. C. Tiwari, G. K. Nagar, et al. 2015. Pathophysiological mechanism of bone loss in type 2 diabetes involves inverse regulation of osteoblast function by PGC-1α and skeletal muscle atrogenes: AdipoR1 as a potential target for reversing diabetes-induced osteopenia. *Diabetes* 64: 2609–2623.
25. Garimella, M. G., S. Kour, V. Piprode, M. Mittal, A. Kumar, L. Rani, S. T. Pote, G. C. Mishra, N. Chattopadhyay, and M. R. Wani. 2015. Adipose-Derived Mesenchymal Stem Cells Prevent Systemic Bone Loss in Collagen-Induced Arthritis. *J. Immunol.* 195: 5136–5148.
26. Bouxsein, M. L., S. K. Boyd, B. A. Christiansen, R. E. Guldberg, K. J. Jepsen, and R. Müller. 2010. Guidelines for assessment of bone microstructure in rodents using micro-computed tomography. *J. Bone Miner. Res.* 25: 1468–1486.
27. Pritzker, K. P., S. Gay, S. A. Jimenez, K. Ostergaard, J. P. Pelletier, P. A. Revell, D. Salter, and W. B. van den Berg. 2006. Osteoarthritis cartilage histopathology: grading and staging. *Osteoarthritis Cartilage* 14: 13–29.
28. Pfander, D., N. Heinz, P. Rothe, H. D. Carl, and B. Swoboda. 2004. Tenascin and aggrecan expression by articular chondrocytes is influenced by interleukin 1beta: a possible explanation for the changes in matrix synthesis during osteoarthritis. *Ann. Rheum. Dis.* 63: 240–244.
29. Kapoor, M., J. Martel-Pelletier, D. Lajeunesse, J. P. Pelletier, and H. Fahmi. 2011. Role of proinflammatory cytokines in the pathophysiology of osteoarthritis. *Nat. Rev. Rheumatol.* 7: 33–42.
30. Li, G., J. Yin, J. Gao, T. S. Cheng, N. J. Pavlos, C. Zhang, and M. H. Zheng. 2013. Subchondral bone in osteoarthritis: insight into risk factors and microstructural changes. *Arthritis Res. Ther.* 15: 223.
31. Aigner, T., S. Söder, P. M. Gebhard, A. McAlinden, and J. Haag. 2007. Mechanisms of disease: role of chondrocytes in the pathogenesis of osteoarthritis–structure, chaos and senescence. *Nat. Clin. Pract. Rheumatol.* 3: 391–399.
32. Strassle, B. W., L. Mark, L. Leventhal, M. J. Piesla, X. Jian Li, J. D. Kennedy, S. S. Glasson, and G. T. Whiteside. 2010. Inhibition of osteoclasts prevents cartilage loss and pain in a rat model of degenerative joint disease. *Osteoarthritis Cartilage* 18: 1319–1328.
33. de Groot, R. P., P. J. Coffer, and L. Koenderman. 1998. Regulation of proliferation, differentiation and survival by the IL-3/IL-5/GM-CSF receptor family. *Cell. Signal.* 10: 619–628.
34. McKinstry, W. J., C. L. Li, J. E. Rasko, N. A. Nicola, G. R. Johnson, and D. Metcalf. 1997. Cytokine receptor expression on hematopoietic stem and progenitor cells. *Blood* 89: 65–71.
35. Budel, L. M., O. Elbaz, H. Hoogerbrugge, R. Delwel, L. A. Mahmoud, B. Löwenberg, and I. P. Touw. 1990. Common binding structure for granulocyte macrophage colony-stimulating factor and interleukin-3 on human acute myeloid leukemia cells and monocytes. *Blood* 75: 1439–1445.
36. Barhanpurkar, A. P., N. Gupta, R. K. Srivastava, G. B. Tomar, S. P. Naik, S. R. Joshi, S. T. Pote, G. C. Mishra, and M. R. Wani. 2012. IL-3 promotes osteoblast differentiation and bone formation in human mesenchymal stem cells. *Biochem. Biophys. Res. Commun.* 418: 669–675.
37. Billinghurst, R. C., L. Dahlberg, M. Ionescu, A. Reiner, R. Bourne, C. Rorabeck, P. Mitchell, J. Hambor, O. Diekmann, H. Tschesche, et al. 1997. Enhanced cleavage of type II collagen by collagenases in osteoarthritic articular cartilage. *J. Clin. Invest.* 99: 1534–1545.
38. Little, C. B., A. Barai, D. Burkhardt, S. M. Smith, A. J. Fosang, Z. Werb, M. Shah, and E. W. Thompson. 2009. Matrix metalloproteinase 13-deficient mice are resistant to osteoarthritic cartilage erosion but not chondrocyte hypertrophy or osteophyte development. *Arthritis Rheum.* 60: 3723–3733.
39. Troeberg, L., and H. Nagase. 2012. Proteases involved in cartilage matrix degradation in osteoarthritis. *Biochim. Biophys. Acta* 1824: 133–145.
40. Lee, A. S., M. B. Ellman, D. Yan, J. S. Kroin, B. J. Cole, A. J. van Wijnen, and H. J. Im. 2013. A current review of molecular mechanisms regarding osteoarthritis and pain. *Gene* 527: 440–447.
41. Moodie, J. P., K. S. Stok, R. Müller, T. L. Vincent, and S. J. Shefelbine. 2011. Multimodal imaging demonstrates concomitant changes in bone and cartilage after destabilisation of the medial meniscus and increased joint laxity. *Osteoarthritis Cartilage* 19: 163–170.
42. Pan, J., B. Wang, W. Li, X. Zhou, T. Scherr, Y. Yang, C. Price, and L. Wang. 2012. Elevated cross-talk between subchondral bone and cartilage in osteoarthritic joints. *Bone* 51: 212–217.
43. Zhang, L. Z., H. A. Zheng, Y. Jiang, Y. H. Tu, P. H. Jiang, and A. L. Yang. 2012. Mechanical and biologic link between cartilage and subchondral bone in osteoarthritis. *Arthritis Care Res. (Hoboken)* 64: 960–967.

NATURE REVIEWS RHEUMATOLOGY | RESEARCH HIGHLIGHT

EXPERIMENTAL ARTHRITIS

A protective role for IL-3 in mouse OA

Joanna Collison

Nature Reviews Rheumatology **12**, 374–375 (2016) doi:10.1038/nrrheum.2016.96
Published online 03 June 2016

Subject terms: Cartilage Chondrocytes Experimental models of disease Osteoarthritis

NPG

In a mouse model of post-traumatic osteoarthritis (OA), Mohan Wani and colleagues show that intra-articular injection of IL-3 (a cytokine released by activated T cells) limits damage to cartilage and bone. “IL-3 has a multifaceted role in amelioration of cartilage and subchondral bone damage,” asserts Wani, “in addition to modulating the inflammatory response associated with OA.”

Previously, these researchers found that IL-3 inhibits osteoclast differentiation *in vitro*, and has indirect, protective effects on cartilage and bone damage in mouse models of inflammatory arthritis.

In the current study, Wani and colleagues showed that the receptor for IL-3 is highly expressed on both mouse and human primary chondrocytes. Under nonpathological conditions, exogenous IL-3 did not affect chondrocyte proliferation, gene expression, or matrix synthesis, nor did its presence affect the differentiation of chondrocytes from cultured human mesenchymal stem cells. By contrast, in the presence of the proinflammatory cytokine IL-1β, IL-3 was able to increase the expression of the chondrocyte specific genes *Sox9* and *Col2a*, which are downregulated by IL-1β in mouse chondrocytes. The presence of IL-3 was also able to reduce the upregulation of the genes encoding matrix metalloproteinases MMP-3 and MMP-13 caused by IL-1β and TNF in both mouse and human chondrocytes. Thus, IL-3 seems to mainly reduce cartilage damage by downregulating the expression of MMPs.

Moving to an anterior cruciate ligament transection mouse model of post-traumatic OA, Wani and colleagues showed that intra-articular administration of IL-3 was effective in attenuating cartilage breakdown, irrespective of whether the cytokine treatment was started before or after the development of OA. Both treatment protocols were able to reduce articular cartilage damage and improve damaged subchondral bone architecture.

“intra-articular administration of IL-3 was effective in attenuating cartilage breakdown”

According to Wani, “IL-3 has therapeutic potential in amelioration of degeneration of articular cartilage and

subchondral bone microarchitecture associated with OA." The team are now planning to conduct studies into the role of IL-3 treatment in a large-animal (dog) model of OA.

References

1. Kour, S. *et al*. IL-3 decreases cartilage degeneration by downregulating matrix metalloproteinases and reduces joint destruction in osteoarthritic mice. *J. Immunol.* http://dx.doi.org/10.4049/jimmunol.1500907 (2016)

Download references

More Research Highlights

EXPERIMENTAL ARTHRITIS
Helminth infection ameliorates arthritis

IN BRIEF
Digital ulcers unaffected by endothelin blockade

IN BRIEF
Immunosuppressive therapies and cancer risk

IN BRIEF
Tocilizumab safe and effective for PMR

INFLAMMATORY MYOPATHIES
Muscle pathology helps predict JDM outcomes

SYSTEMIC SCLEROSIS
Tenascin C perpetuates tissue fibrosis

LUPUS NEPHRITIS
Targeting Bcl-2 prevents nephritis in mice

SYSTEMIC LUPUS ERYTHEMATOSUS
SHP2 inhibition ameliorates disease in lupus-prone mice

Nature Reviews Rheumatology ISSN 1759-4790 EISSN 1759-4804

IL-3 Differentially Regulates Membrane and Soluble RANKL in Osteoblasts through Metalloproteases and the JAK2/STAT5 Pathway and Improves the RANKL/OPG Ratio in Adult Mice

Kanupriya Singh, Vikrant Piprode, Suhas T. Mhaske, Amruta Barhanpurkar-Naik, and Mohan R. Wani

Bone remodeling comprises balanced activities between osteoclasts and osteoblasts, which is regulated by various factors, including hormones and cytokines. We previously reported that IL-3 inhibits osteoclast differentiation and pathological bone loss. IL-3 also enhances osteoblast differentiation and bone formation from mesenchymal stem cells. However, the role of IL-3 in regulation of osteoblast–osteoclast interactions and underlying mechanisms is not yet delineated. In this study, we investigated the role of IL-3 on the regulation of osteoblast-specific molecules, receptor activator of NF-κB ligand (RANKL), and osteoprotegerin (OPG) that modulate bone homeostasis. We found that IL-3 increases RANKL expression at both the transcriptional and translational levels, and it showed no effect on OPG expression in calvarial osteoblasts. The increased RANKL expression by IL-3 induces mononuclear osteoclasts; however, it does not induce multinuclear osteoclasts. Interestingly, IL-3 decreases soluble RANKL by reducing ectodomain shedding of membrane RANKL through downregulation of metalloproteases mainly a disintegrin and metalloproteinase (ADAM)10, ADAM17, ADAM19, and MMP3. Moreover, IL-3 increases membrane RANKL by activating the JAK2/STAT5 pathway. Furthermore, IL-3 enhances RANKL expression in mesenchymal stem cells of wild-type mice but not in STAT5a knockout mice. Interestingly, IL-3 restores RANKL expression in adult mice by enhancing bone-specific RANKL and decreasing serum RANKL. Furthermore, IL-3 increases the serum OPG level in adult mice. Thus, our results reveal, to our knowledge for the first time, that IL-3 differentially regulates two functional forms of RANKL through metalloproteases and the JAK2/STAT5 pathway, and it helps in restoring the decreased RANKL/OPG ratio in adult mice. Notably, our studies indicate the novel role of IL-3 in regulating bone homeostasis in important skeletal disorders. ***The Journal of Immunology*****, 2018, 200: 595–606.**

Bone maintains its structural and functional integrity by the physiological process of bone remodeling, which is regulated by interactions between bone-resorbing osteoclasts and bone-forming osteoblasts. Osteoclasts are derived from hematopoietic stem cells of monocyte/macrophage lineage, and osteoblasts differentiate from mesenchymal stem cells (MSCs) (1). Osteoblasts regulate bone remodeling by producing both stimulatory and inhibitory factors that tightly regulate osteoclast formation and activity. Stimulatory factors include glycoproteins such as M-CSF and receptor activator of NF-κB (RANK) ligand (RANKL) (2–4). RANKL is also expressed by various cell types such as activated T cells (5, 6), mesenchymal cells (7), keratinocytes (8), B lymphocytes (9, 10), mammary epithelial cells (11), vascular endothelial cells (12), cancer cells (13), and microglia (14). RANKL is a 35-kDa protein found both as a transmembrane glycoprotein on the surface of cells and secreted soluble protein. Binding of RANKL to its receptor RANK on the surface of osteoclast precursors initiates signals (15), which lead to fusion, maturation, survival, and activation of osteoclasts (16, 17). Osteoblasts also secrete inhibitory protein known as osteoprotegerin (OPG), which is a decoy receptor for RANKL that prevents the binding of RANKL to RANK, thereby inhibiting osteoclast differentiation and activation (18).

Any alterations in the RANKL/OPG ratio modulate the bone remodeling in skeletal diseases such as osteoporosis, Paget disease, and osteoarthritis (19). The age-related bone loss due to systemic changes, including growth factors, sex steroids, and parathyroid hormone, may modulate RANKL and OPG expression in vivo (20). It has been reported that an increase in serum parathyroid hormone level with postmenopausal aging causes stimulation of RANKL and inhibition of OPG expression (21, 22). These findings indicate that regulation of RANKL and OPG is very important for the prevention and treatment of bone loss in skeletal diseases and also in aging.

Cytokines secreted by immune and other cell types play an important role in regulation of bone remodeling (23). Previously, we reported that IL-3, a cytokine secreted by activated T cells (24), is a potent inhibitor of osteoclastogenesis and inhibits both RANKL and TNF-α–induced osteoclast formation and bone resorption (25–28). IL-3 also increases in vitro osteoblast differentiation and matrix mineralization from human MSCs, and it enhances ectopic bone formation in immunocompromised mice (29). Precise equilibrium between osteoblast and osteoclast activity is crucial to maintain the structural and functional integrity of bone, which is regulated by

National Centre for Cell Science, Savitribai Phule Pune University Campus, Ganeshkhind, Pune 411007, India

ORCIDs: 0000-0003-3511-1459 (K.S.); 0000-0002-5672-1355 (S.T.M.).

Received for publication August 31, 2016. Accepted for publication November 5, 2017.

This work was supported by the Department of Biotechnology under Government of India Grant BT/HRD/34/01/2009 (to M.R.W.) and K.S. received a Senior Research Fellowship from the Council of Scientific and Industrial Research (New Delhi, India).

Address correspondence and reprint requests to Dr. Mohan R. Wani, National Centre for Cell Science, Savitribai Phule Pune University Campus, Ganeshkhind, Pune 411007, India. E-mail address: mohanwani@nccs.res.in

The online version of this article contains supplemental material.

Abbreviations used in this article: ADAM, a disintegrin and metalloproteinase; AT-MSC, adipose tissue–derived MSC; ΔMFI, change in mean fluorescence intensity; MSC, mesenchymal stem cell; OPG, osteoprotegerin; RANK, receptor activator of NF-κB; RANKL, RANK ligand; TRAP, tartrate-resistant acid phosphatase.

RANKL and OPG (30). In this study, we investigated the role of IL-3 in modulation of RANKL and OPG expression in mouse calvarial osteoblasts and also in adult mice.

We found that IL-3 increases the expression of membrane-bound RANKL and decreases secretion of soluble RANKL in vitro in calvarial osteoblasts. The expression of OPG in osteoblasts was not affected by IL-3. Furthermore, IL-3 decreases soluble RANKL in osteoblasts by downregulation of metalloproteases, a disintegrin and metalloproteinases (ADAMs) such as ADAM10, ADAM17, ADAM19, and MMP3, and it increases membrane-bound RANKL by activating the JAK2/STAT5 pathway. Interestingly, IL-3 improves the disturbed RANKL/OPG ratio in serum of adult mice. Thus, IL-3 differentially regulates two functional forms of RANKL in both in vitro and in vivo conditions.

Materials and Methods

Animals

BALB/c mice of 2–5 d, 6–8 wk, 3 mo, and 1 y old were obtained from the Experimental Animal Facility of the National Centre for Cell Science (Pune, India). STAT5a [C.129S (B6)-*Stat5a*^{tm1Mam}/J] and STAT5b (C.129-*Stat5b*^{tm1Hwd}/J) knockout mice were obtained from The Jackson Laboratory. Water and food were provided ad libitum. All protocols involving animal use were approved by an Institutional Animal Ethics Committee.

Reagents and culture conditions

RANKL Ab and fluorochrome-conjugated secondary Abs were obtained from Abcam. Polyclonal Abs for IL-3Rα, OPG, pERK1/2, ERK1/2, pJAK2, JAK2, pSTAT5a/b, STAT5, and β-actin were obtained from Santa Cruz Biotechnology. The HRP-conjugated secondary Abs were from Bangalore Genei. Fluorochrome-conjugated anti-mouse RANKL (clone IK22/5) and anti-mouse IL-3Rα (clone 5B11) Abs were obtained from BioLegend. Recombinant mouse IL-3 was obtained from BD Biosciences. 1α,25-Dihydroxyvitamin D_3 was obtained from Sigma-Aldrich. FCS, L-glutamine, TRIzol reagent, cDNA synthesis kit, and SYBR Green were obtained from Invitrogen. Collagenase and dispase were purchased from MP Biomedicals. RANKL and OPG ELISA kits were obtained from R&D Systems.

All cultures were incubated in growth medium containing α-MEM, heat-inactivated FCS (10%), L-glutamine (2 mM), penicillin (100 IU/ml), streptomycin (100 μg/ml), and osteogenic factors β-glycerophosphate (10 mM) and ascorbic acid (50 μg/ml, all from Sigma-Aldrich). All incubations were performed at 37˚C in a humidified atmosphere of 5% CO_2 in air.

Isolation of calvarial osteoblasts

Mouse calvarial osteoblasts were isolated from 2- to 5-d-old BALB/c mice using a modified sequential digestion method as described previously (31). Briefly, surgically resected calvariae were cleaned off adherent soft tissues and subjected to five sequential (5, 15, 10, 10, and 5 min) digestions in enzyme solution containing 0.1% collagenase and 0.2% dispase at 37˚C. Cells released from second to fourth digestions were pooled, centrifuged, and resuspended in growth medium as described above. Calvarial osteoblasts of passage 2 were used in all experiments.

Isolation of bone marrow–derived osteoclast precursors

The stromal cell–free and M-CSF–dependent osteoclast precursors were isolated from 6- to 8-wk-old BALB/c mice as previously described (25). Briefly, femoral and tibial bones were aseptically removed and cleaned by removing adherent soft tissues. The bone ends were cut, and the bone marrow cavity was flushed out with α-MEM from one end of the bone using a sterile 21-gauge needle. Bone marrow cells were washed twice and incubated for 24 h in the presence of M-CSF (10 ng/ml) at a density of 3×10^5 cells/ml in a 75-cm^2 flask. After 24 h, nonadherent cells were collected and layered on a Ficoll-Hypaque (Sigma-Aldrich) gradient. Cells at the gradient interface were collected, washed twice, and used for further experiments.

Coculture model for osteoclastogenesis

To evaluate the effect of IL-3 on osteoclast differentiation in a coculture model, mouse calvarial osteoblasts (2×10^4 cells per well) and bone marrow–derived osteoclast precursors (2×10^5 cells per well) were cocultured in 48-well plates containing α-MEM and 10% FCS with or without IL-3 for 7 d (32). Vitamin D_3 was used as positive regulator of osteoclastogenesis in a coculture system that is known to increase RANKL expression on osteoblasts. Osteoclast formation was evaluated by tartrate-resistant acid phosphatase (TRAP) staining.

Isolation of adipose tissue–derived MSCs

Mouse adipose tissue–derived MSCs (AT-MSCs) were isolated from 10- to 12-wk-old wild-type, STAT5a, and STAT5b knockout mice as described previously (33). Briefly, s.c. adipose tissue was digested with 2 mg/ml collagenase (type 1A; Sigma-Aldrich) in PBS at 37˚C for 15–20 min. The cell suspension obtained was centrifuged, resuspended in α-MEM containing 10% FCS, and seeded in a culture flask. After 72 h nonadherent cells were discarded and adherent cells were cultured until they attained 80–90% confluency. Homogeneous populations of AT-MSCs from passage 2 or 3 were used in all further experiments.

MTT assay

The proliferation of mouse calvarial osteoblasts in the presence of IL-3 was examined using an MTT assay. After the incubation period, cell culture media were replaced with 100 μl of MTT (0.5 mg/ml) solution and cells were further incubated at 37˚C for 3–4 h. The MTT solution was removed and formazan crystals formed were dissolved in 100 μl of DMSO. The absorbance was measured at 570 nm.

Quantitative real-time PCR

Expression of RANKL, OPG, M-CSF, ADAM10, ADAM17, ADAM19, MMP3, MMP14, TRAP, cathepsin K, calcitonin receptor, integrin β_3 and GAPDH was assessed by real-time PCR analysis. RNA was isolated from cells by the TRIzol reagent method (Invitrogen). Two micrograms of total RNA was used for synthesis of cDNAs by reverse transcription (cDNA synthesis kit). For real-time PCR, a 10-μl reaction mixture containing SYBR Green and 10 pmol of each primer were used and PCR was set using the StepOnePlus system (Applied Biosystems). The amplification was performed using one cycle of 95˚C for 10 min and 40 cycles of denaturation at 95˚C for 15 s, primer annealing and extension at 60˚C for 60 s, followed by melt curve analysis. The primer sequences (IDT) used are summarized in Supplemental Table I. Each reaction was run in duplicates and data were analyzed for fold change using the comparative $2^{-\Delta\Delta Ct}$ method.

Immunofluorescence microscopy

Mouse calvarial osteoblasts were cultured on glass coverslips in 24-well plates in the absence or presence of IL-3 for the indicated time points. The cells were washed twice with PBS, fixed with 4% paraformaldehyde for 10 min, and permeabilized with 0.1% Triton X-100 in PBS for 5 min. Staining for RANKL, OPG and IL-3Rα was carried out using primary Abs followed by fluorochrome-conjugated secondary Abs. After washing cells were mounted using Dabco (Sigma-Aldrich) and viewed with a Zeiss LSM 510 confocal microscope equipped with argon and helium lasers.

Flow cytometry

Cells were cultured with or without IL-3 for the indicated time points. At the end of the culture period adherent cells were harvested from culture dishes using cell dissociation buffer (Life Technologies), and the few remaining cells were dislodged by gentle scraping on ice. Cell surface staining was performed by incubating 10^5 cells in 100 μl of PBS with fluorochrome-conjugated Abs. For intracellular staining, cells were first permeabilized with permeabilization buffer (0.1% Triton X-100 in 1× PBS) and then stained with RANKL and OPG Abs. Cells were washed, acquired, and analyzed with a BD FACSCalibur. Data were analyzed using CellQuest Pro software (Becton-Dickinson). The results are expressed as the percentage of cells and the change in mean fluorescence intensity (ΔMFI).

ELISA

Cell culture supernatants were harvested after the indicated time of incubation, centrifuged, and immediately frozen at −80˚C until further analysis. All samples were thawed immediately prior to evaluation by ELISA. Soluble RANKL and OPG proteins were measured in supernatant and serum using the respective Quantikine mouse ELISA kits. The procedure was carried out according to the manufacturer's instructions and the absorbance was measured at 450 nm with a correction wavelength of 540 nm.

Western blotting

Cells were seeded at a density of 5×10^4 cells/cm^2 in α-MEM containing 10% FCS and cultured for the indicated time periods in the absence or presence of IL-3. The cells were lysed in RIPA buffer containing protease

inhibitors, and proteins were estimated using the BCA method. Protein samples were then subjected to 12% SDS-PAGE. The proteins were transferred from gels onto a nitrocellulose membrane for immunoblot analysis. Blocking was performed with 5% nonfat dry milk in TBS buffer. The membrane was then incubated with primary Ab (1:1000) for 3 h. After washing, the membranes were incubated with HRP-conjugated secondary Abs, and labeled proteins were detected using ECL reagents (Amersham Biosciences). Relative intensities of protein bands were analyzed by densitometry using ImageJ software.

TRAP staining

Cells were washed gently in PBS and fixed in 10% formalin for 10 min at room temperature. TRAP staining was performed at 37°C for 10–15 min by incubating cells in TRAP buffer (70 mM sodium acetate, 30 mM acetic acid, 0.1 mg/ml napthol AS-MX phosphate disodium salt, 0.1% Triton X-100 at pH 5). The number of TRAP-positive mononuclear and multinuclear (three or more nuclei) osteoclasts was counted.

In vivo analysis of RANKL and OPG

To investigate the in vivo role of IL-3 on RANKL and OPG expression, young mice of 3 mo old and adult mice of 1 y old were used. Adult mice were injected i.p. with PBS or IL-3 (3 μg per mouse per day) for 5 d. Young mice injected with PBS were used as a control to compare the changes in RANKL and OPG with adult mice. On day 6, bone and serum samples were collected. Bone-specific RANKL expression was analyzed by immunoblotting from femur and tibia after removal of bone marrow. Serum RANKL and OPG levels were analyzed by ELISA.

Statistical analysis

Results are represented as mean ± SEM. Statistical significance was calculated using one-way ANOVA with a subsequent post hoc Bonferroni test for multiple comparisons. A p value <0.05 was considered significant.

Results

IL-3 enhances RANKL expression in calvarial osteoblasts

To investigate the role of IL-3 on RANKL and OPG expression we first confirmed the expression of IL-3Rα on mouse calvarial osteoblasts. Calvarial osteoblasts showed expression of IL-3Rα as analyzed by immunofluorescence and Western blotting (Supplemental Fig. 1A, 1B). To further quantify IL-3Rα expression on osteoblasts, we performed flow cytometry analysis and observed that ~48.97% cells were positive for IL-3Rα expression (Supplemental Fig. 1C). To evaluate the effect of IL-3 on RANKL and OPG in a time-dependent manner, we cultured calvarial osteoblasts for 12, 24, 48, and 72 h in osteogenic media containing β-glycerophosphate

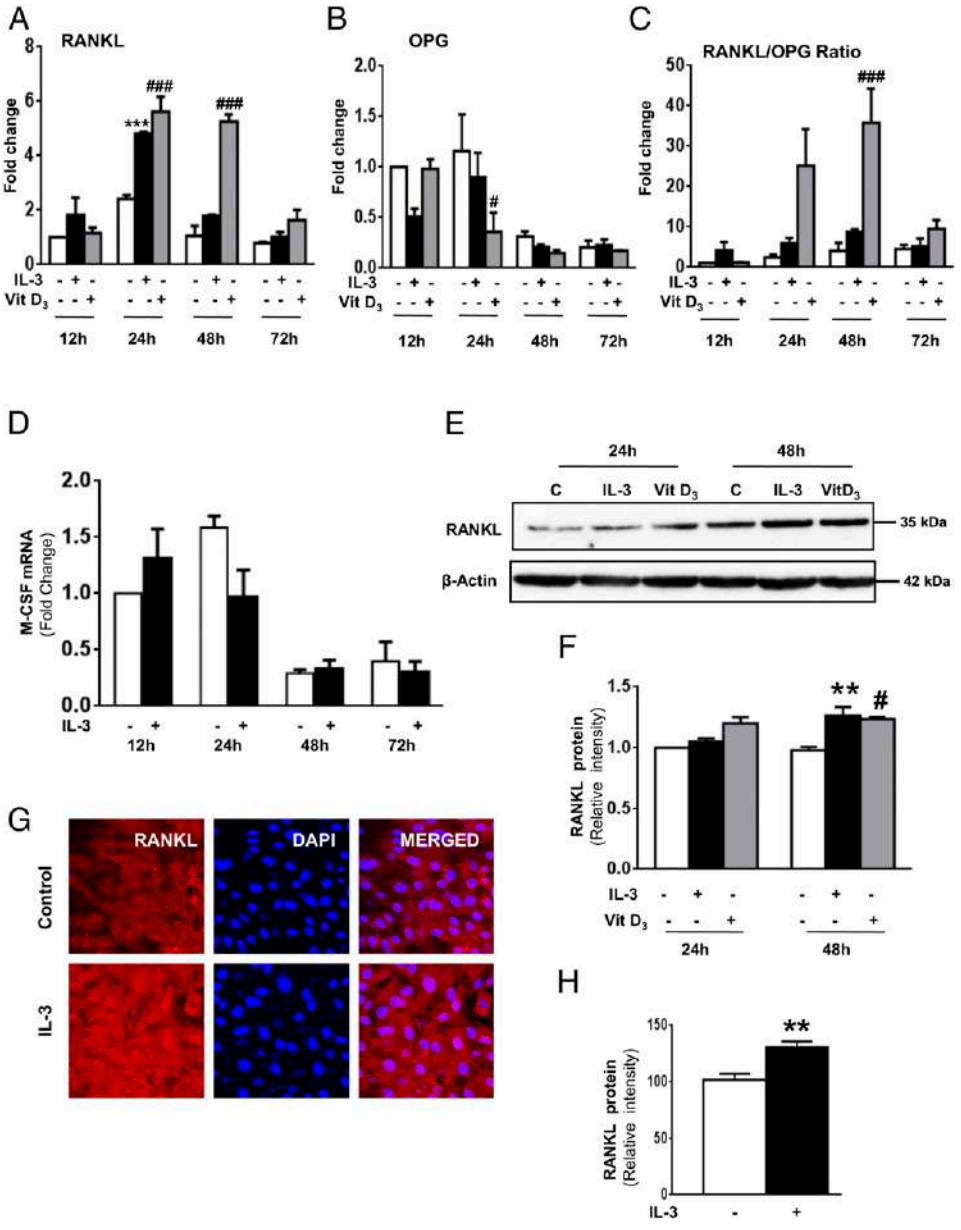

FIGURE 1. IL-3 upregulates RANKL expression both at the gene and protein levels. Mouse calvarial osteoblasts were cultured for 12, 24, 48, and 72 h in α-MEM containing β-glycerophosphate (10 mM) and ascorbic acid (50 μg/ml) in the absence or presence of recombinant mouse IL-3 (100 ng/ml) or vitamin D_3 (10^{-8} M) and gene expression of RANKL (**A**), OPG (**B**), and M-CSF (**D**) was determined by quantitative PCR. Results in (A), (B), and (D) are expressed as fold change of control. (**C**) Ratio of quantitative values of RANKL and OPG genes. Cells were cultured for 24 and 48 h in the absence or presence of IL-3 or vitamin D_3 and RANKL expression was analyzed by Western blotting (**E**), and relative intensities (**F**) were calculated by densitometry using ImageJ software. (**G**) Total RANKL protein expression was evaluated by immunofluorescence by culturing cells for 48 h in the absence or presence of IL-3. Original magnification, ×63. (**H**) Fluorescence intensity of RANKL expression was measured by using ImageJ software. Bar graphs are expressed as mean ± SEM of three independent experiments. Significance was calculated by a one-way ANOVA followed by a post hoc Bonferroni multiple comparison test. $^{**}p < 0.01$, $^{***}p < 0.001$, IL-3 versus untreated controls. $^{\#}p < 0.05$, $^{\#\#\#}p < 0.001$, vitamin D_3 versus untreated controls.

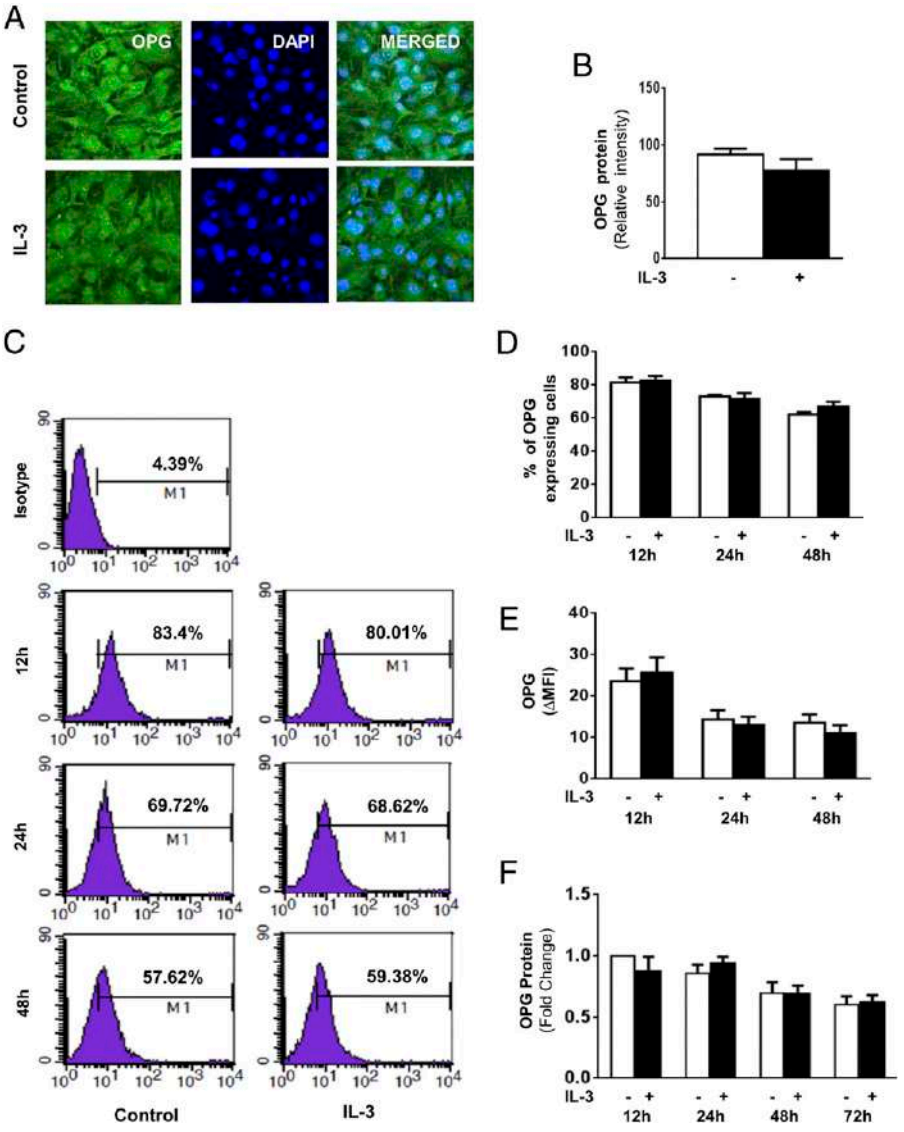

FIGURE 2. Effect of IL-3 on OPG protein expression. (**A**) OPG protein expression was evaluated by immunofluorescence by culturing osteoblasts for 48 h in the absence or presence of IL-3. Original magnification ×63. (**B**) Fluorescence intensity of RANKL expression was measured by using ImageJ software. (**C**) Calvarial osteoblasts were incubated for 12, 24, and 48 h in the absence or presence of IL-3 (100 ng/ml) and analysis of intracellular OPG protein was done by flow cytometry. The data are representative of three independent experiments. (**D** and **E**) Average percentages of OPG-expressing cells and ΔMFI of three independent experiments. Bar graphs are expressed as mean ± SEM of three independent experiments. (**F**) Cells were incubated for 12, 24, 48, and 72 h with IL-3 and secretion of OPG in culture supernatant was examined by ELISA. Results are the average of four independent experiments.

(10 mM) and ascorbic acid (50 μg/ml) in the absence or presence of IL-3 (100 ng/ml) or vitamin D_3 (10^{-8} M), and expression of RANKL and OPG was examined by quantitative real-time PCR. Vitamin D_3 was used as a positive stimulator of RANKL expression. It was observed that vitamin D_3 significantly enhanced RANKL expression at 24 and 48 h and IL-3 significantly increased RANKL expression at 24 h (Fig. 1A). Vitamin D_3 significantly decreased OPG expression at 24 h. However, IL-3 did not show any effect on OPG expression at all time points (Fig. 1B). We further observed that vitamin D_3 significantly increased the RANKL/OPG ratio at 48 h. However, IL-3 did not show any significant effect on the RANKL/OPG ratio (Fig. 1C). We further evaluated whether IL-3 has any role in regulation of another glycoprotein, M-CSF, which is also secreted by osteoblasts and required for survival and early stages of osteoclast differentiation. Similar to OPG, IL-3 showed no effect on expression of M-CSF at all time points (Fig. 1D).

To rule out the possibility that osteogenic factors could induce RANKL expression in osteoblasts, we evaluated the dose-dependent effect of IL-3 on RANKL and OPG expression in the absence of osteogenic factors. Cells were cultured for 24 h with various concentrations of IL-3 in the absence of osteogenic factors, and the expression of RANKL and OPG was analyzed by real-time PCR. We found that IL-3 increased the RANKL expression and showed no effect on OPG (Supplemental Fig. 2A, 2B). These results suggested that the effect of IL-3 on RANKL expression is direct and not through osteogenic factors. However, to mimic an in vivo–like situation we used osteogenic factors in all further experiments.

Next, to examine the effect of IL-3 on RANKL at the protein level, osteoblasts were cultured for 24 and 48 h with IL-3 or vitamin D_3, and expression of RANKL was evaluated by immunoblotting and the relative intensity was analyzed by ImageJ software. It was observed that vitamin D_3 significantly increased RANKL expression at 48 h. Similar to vitamin D_3, IL-3 also increased RANKL expression significantly at 48 h (Fig. 1E, 1F). To further confirm the effect of IL-3 on RANKL protein, we evaluated total protein expression at 48 h by immunofluorescence microscopy. IL-3 significantly enhanced RANKL expression at the protein level (Fig. 1G). Fig. 1H shows the fluorescence intensity of RANKL analyzed by ImageJ software. All of these results suggest that IL-3 significantly increases RANKL at both the gene and protein levels. We also observed that IL-3 has no effect on proliferation of osteoblasts in a dose- and time-dependent manner, and also IL-3 was not toxic to the cells at 100 ng/ml concentration (Supplemental Fig. 3).

Effect of IL-3 on functional forms of OPG and RANKL

OPG is a decoy receptor for RANKL and the only member of TNF receptor superfamily, which is a secretary protein (18). Because IL-3

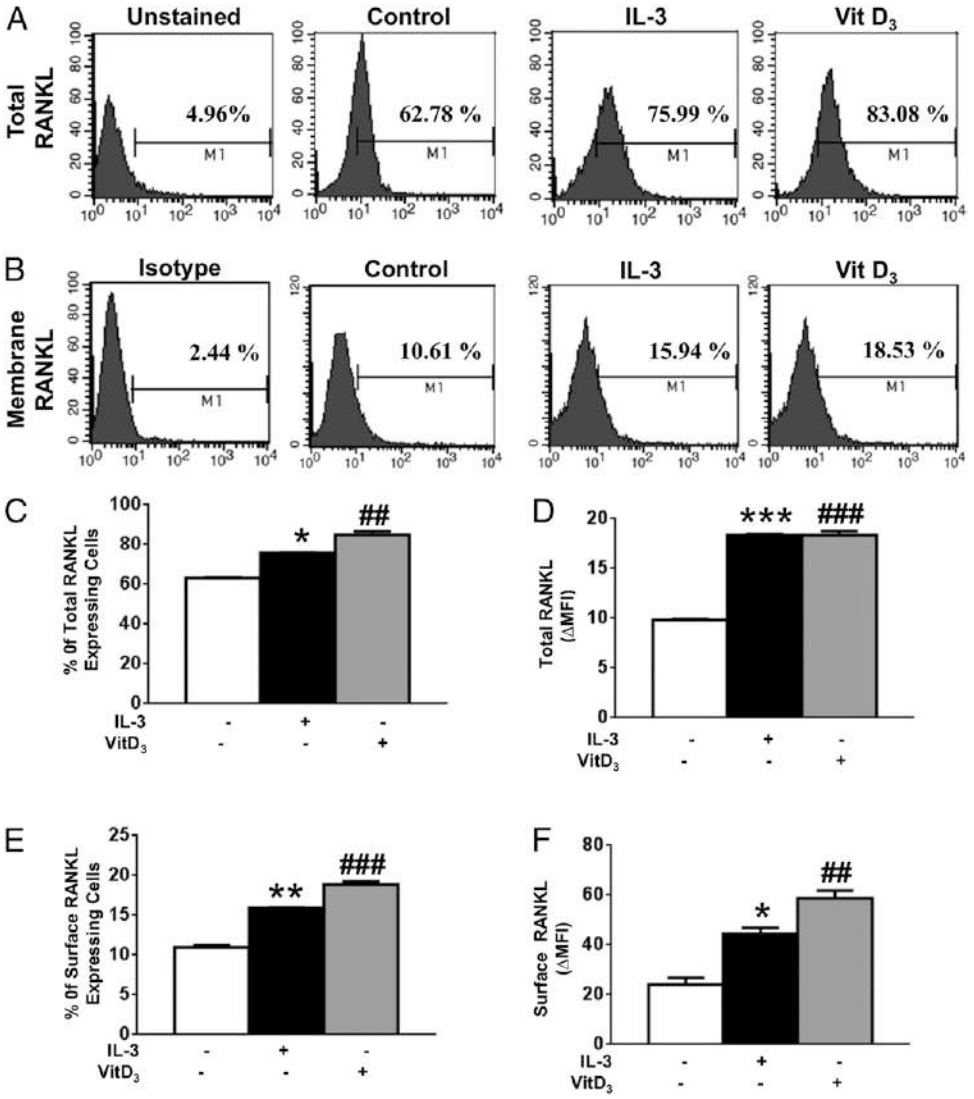

FIGURE 3. IL-3 enhances membrane RANKL expression on osteoblasts. Calvarial osteoblasts were incubated with IL-3 or vitamin D_3 for 48 h, and total (**A**) and membrane-bound (**B**) RANKL expression was analyzed by flow cytometry. (**C** and **D**) Average percentages of cells and ΔMFI of total RANKL. (**E** and **F**) Average percentages of cells and ΔMFI of membrane-bound RANKL. Data are representative of three independent experiments. $^{*}p < 0.05$, $^{**}p < 0.01$, $^{***}p < 0.001$, IL-3 versus untreated controls. $^{\#\#}p < 0.01$, $^{\#\#\#}p < 0.001$, vitamin D_3 versus untreated controls.

showed no effect on OPG at the gene level, we further confirmed the effect of IL-3 on OPG expression at the protein level. OPG protein was evaluated by immunofluorescence by culturing osteoblasts for 48 h with IL-3, as well as with flow cytometry by culturing cells for 12, 24, and 48 h with IL-3. Fig. 2A and 2C show that IL-3 has no effect on OPG expression at the protein level. Fig. 2B represents fluorescence intensity of OPG protein expression. Fig. 2D and 2E show the average percentage of OPG-expressing cells and ΔMFI, respectively. Furthermore, the effect of IL-3 on the functional secretary form of OPG was evaluated by incubating osteoblasts for 12, 24, 48, and 72 h with IL-3, and OPG secretion in the culture supernatant was analyzed by ELISA. IL-3 showed no effect on OPG secretion at all time points (Fig. 2F). These results confirm that IL-3 has no effect on both intracellular and functional OPG expression.

Because IL-3 increased RANKL expression at both the mRNA and protein levels, we further investigated whether this effect of IL-3 on RANKL is sustained at the functional level. Osteoblasts were incubated for 48 h with IL-3 or vitamin D_3, and expression of total and membrane-bound RANKL was analyzed by flow cytometry. We found that both IL-3 and vitamin D_3 significantly increased expression of total and membrane RANKL (Fig. 3A, 3B). Fig. 3C and 3D show the average percentage of cells and ΔMFI of total RANKL. Fig. 3E and 3F shows the average percentage of cells and ΔMFI of membrane-bound RANKL.

IL-3 differentially regulates RANKL expression

RANKL is an osteoclast differentiation factor that stimulates the differentiation, maturation, and activation of osteoclasts from its precursors of monocyte/macrophage lineage. Because IL-3 increases RANKL at both the gene and protein levels, and also increases its membrane expression in osteoblasts, we further evaluated the role of IL-3 in osteoclastogenesis using a coculture model of osteoclast differentiation. Calvarial osteoblasts (2×10^4 cells per well) were cocultured with bone marrow–derived osteoclast precursors (2×10^5 cells per well) in 48-well plates in a contact-dependent manner in the presence of IL-3 (100 ng/ml). Vitamin D_3 (10^{-8} M) was used as positive control for induction of osteoclastogenesis. After 7 d, TRAP-positive mononuclear and multinuclear cells were counted. We observed that vitamin D_3

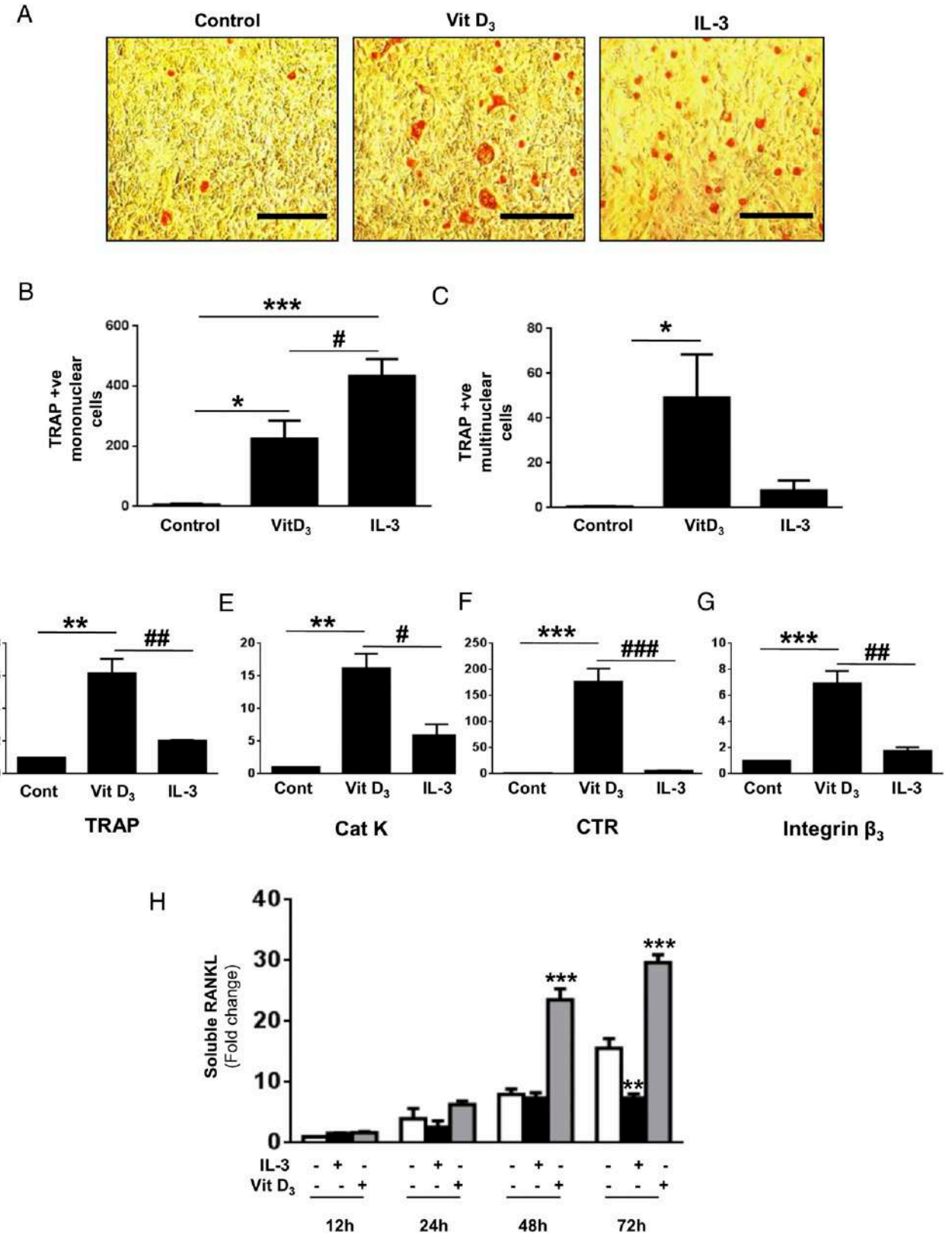

FIGURE 4. Effect of IL-3 on osteoclast formation in coculture model. Mouse calvarial osteoblasts (2×10^4 cells per well) and bone marrow-derived M-CSF–dependent osteoclast precursors (2×10^5 cells per well) were cocultured in 48-well plates in the absence or presence of IL-3 in a contact-dependent manner. (**A**) After 7 d cells were fixed with 10% formalin in PBS and stained for TRAP. Original magnification ×20. Scale bars, 200 μm. TRAP-positive mononuclear (**B**) and multinuclear (**C**) cells were counted. Vitamin D_3 (10^{-8} M) was used as positive control for the induction of osteoclastogenesis. Gene expression analysis of osteoclast-specific markers such as TRAP (**D**), cathepsin K (**E**), calcitonin receptor (**F**), and integrin β_3 (**G**) was done by real-time PCR. (**H**) Calvarial osteoblasts were cultured for 12, 24, 48, and 72 h with IL-3 or vitamin D_3 and secretion of RANKL protein in culture supernatants was analyzed by ELISA. Data are average of two (B and C) or three (D–H) independent experiments. $^*p < 0.05$, $^{**}p < 0.01$, $^{***}p < 0.001$ versus osteogenic media control. $^{\#}p < 0.05$, $^{\#\#}p < 0.01$, $^{\#\#\#}p < 0.001$ IL-3 treated versus vitamin D_3 control.

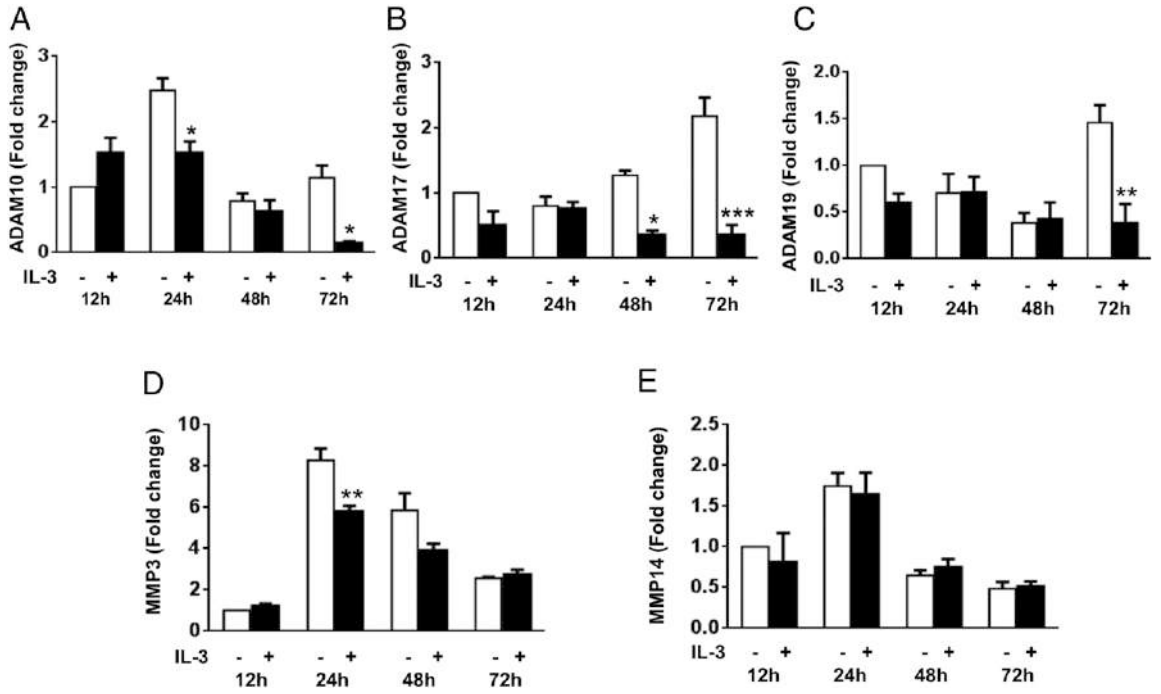

FIGURE 5. IL-3 downregulates the ectodomain shedding of membrane-bound RANKL. Calvarial osteoblasts were incubated for 12, 24, 48, and 72 h with IL-3, and mRNA expression of ADAM10 (**A**), ADAM17 (**B**), ADAM19 (**C**), MMP3 (**D**), and MMP14 (**E**) was examined by real-time PCR. Data are expressed as mean ± SEM, and bar graphs represent the average of three independent experiments. $*p < 0.05$, $**p < 0.01$, $***p < 0.001$ versus untreated controls.

induced formation of both mononuclear and multinuclear TRAP-positive cells (Fig. 4A). IL-3 significantly increased the number of TRAP-positive mononuclear cells (Fig. 4B); however, it was unable to induce formation of TRAP-positive multinuclear osteoclasts (Fig. 4C). We also analyzed the effect of IL-3 on osteoclast-specific genes such as TRAP, cathepsin K, calcitonin receptor, and integrin β_3 in coculture conditions. Vitamin D_3 significantly increased the expression of osteoclast-specific genes; however, IL-3 did not increase the expression of these genes (Fig. 4D–G). These results suggest that despite increasing RANKL expression, IL-3 was unable to induce formation of mature osteoclasts. To investigate the possible reasons for this action of IL-3, we further evaluated the effect of IL-3 on another functional form of RANKL by analyzing the secretion of its soluble form in culture supernatants. Osteoblasts were incubated for 12, 24, 48, and 72 h with IL-3 or vitamin D_3 and soluble RANKL in the culture supernatant was analyzed by ELISA. Vitamin D_3 significantly increased soluble RANKL at 48 and 72 h. Interestingly, we found that IL-3 decreases secretion of soluble RANKL at 24 and 48 h, and significant decrease was seen at 72 h (Fig. 4H). These results suggest that vitamin D_3 increased both functional forms of RANKL. However, IL-3 increases membrane RANKL and decreases its soluble form, and hence it was unable to induce mature osteoclast formation in the coculture model.

Differential regulation of RANKL expression by IL-3 is through metalloproteases

Soluble RANKL is formed by the proteolytic cleavage of membrane-bound RANKL (34, 35). This process is called ectodomain shedding, which is regulated by various ADAMs such as ADAM10, ADAM17, and ADAM19 (34, 36, 37). To further investigate the mechanism of downregulation of soluble RANKL by IL-3, osteoblasts were incubated for 12, 24, 48, and 72 h with IL-3 and mRNA expression of ADAM10, ADAM17, and ADAM19 was examined by real-time PCR. We found that IL-3 significantly downregulated the expression of ADAM10 at 24 and 72 h (Fig. 5A). IL-3 significantly decreased ADAM17 expression at 48 and 72 h, which is the main metalloprotease that regulates production of soluble RANKL from its membrane form (Fig. 5B), and also significantly decreases ADAM19 expression at 72 h (Fig. 5C). Besides ADAMs, MMPs such as MMP3 and MMP14 also play a crucial role in ectodomain shedding of membrane RANKL (38, 39). Therefore, we evaluated the effect of IL-3 on MMP3 and MMP14 expression under similar culture conditions. IL-3 significantly decreases MMP3 expression at 24 h (Fig. 5D) and showed no effect on MMP14 gene expression (Fig. 5E). These results suggest that although IL-3 is capable of increasing RANKL expression at transcript and membrane-bound protein levels, it decreases soluble RANKL by downregulation of metalloproteases that eventually hinder the cleavage of soluble RANKL from its membrane form.

IL-3 activates the JAK2/STAT5 pathway and regulates RANKL expression through STAT5 isoforms

It is well established that among various signaling pathways, JAK2/STAT5 is an important pathway activated by IL-3 (24). To further investigate the molecular mechanism for the increase in membrane RANKL by IL-3, we cultured osteoblasts for 15, 30, 60, and 120 min with IL-3, and activation of JAK2/STAT5 was evaluated by Western blotting. We observed that IL-3 phosphorylates JAK2 at 30, 60, and 120 min and STAT5a/b at 30 and 60 min (Fig. 6A). Besides JAK2, few studies show that ERK1/2 also plays a crucial role in phosphorylation of STAT5 (40). We observed that IL-3 also increases phosphorylation of ERK1/2 in osteoblasts (Fig. 6A). These results indicate that IL-3 stimulates phosphorylation of STAT5 by both JAK2- and ERK1/2-dependent pathways. The STAT5 transcription factor regulates expression of various genes (41). At the functional level not only phosphorylation of STAT5 but also translocation of its phosphorylated form into the nucleus is crucial for its activity. To confirm this we cultured osteoblasts

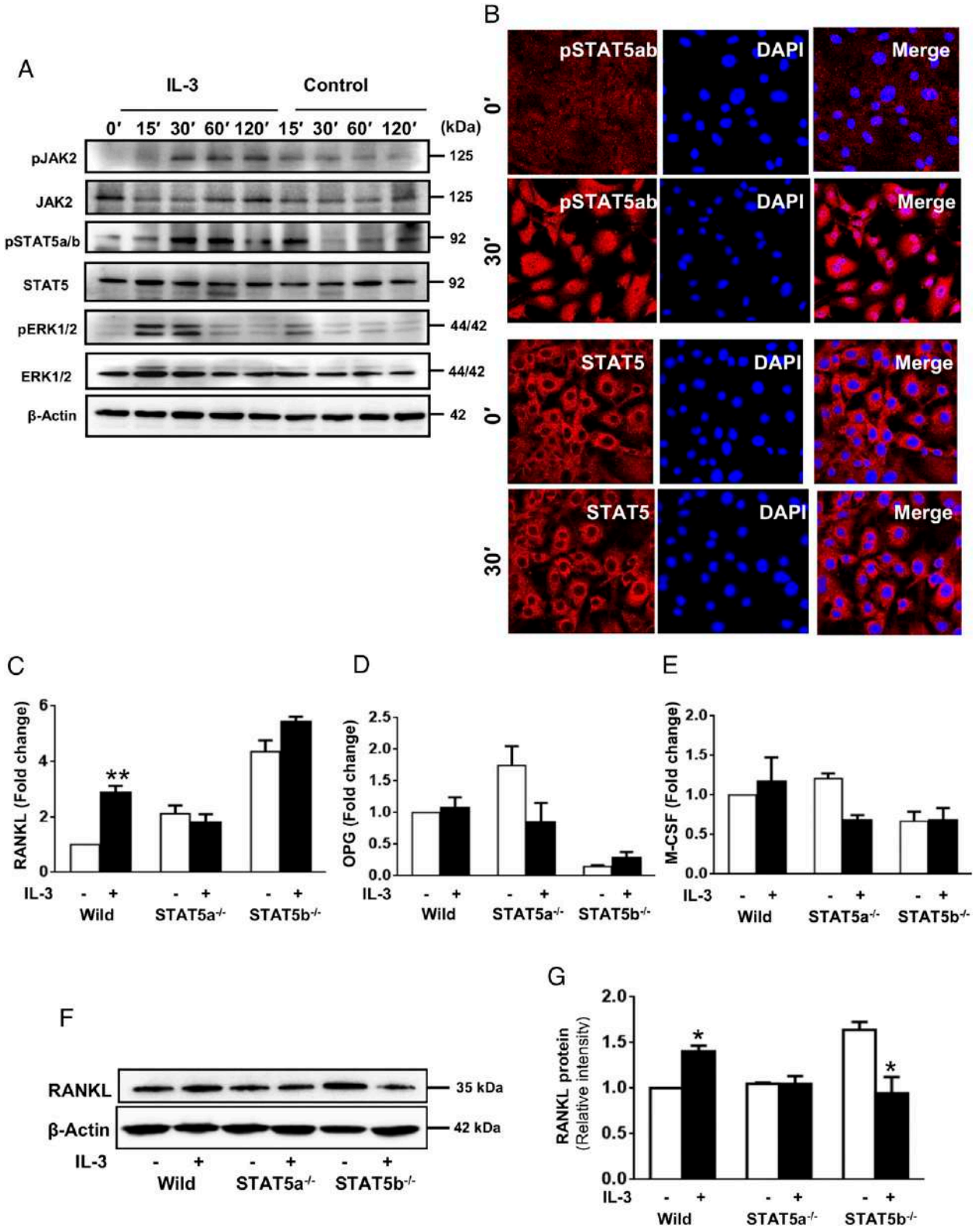

FIGURE 6. IL-3 regulates RANKL expression through the JAK2/STAT5 pathway. Cells were cultured for 0, 15, 30, 60, and 120 min in the presence of IL-3 (100 ng/ml) and activation of JAK2. (**A**) STAT5 and ERK were evaluated by Western blotting. (**B**) Cells were cultured with IL-3 for 30 min and analysis of STAT5 translocation was evaluated by immunofluorescence. Original magnification, ×63. AT-MSCs isolated from wild-type, STAT5a, and STAT5b knockout mice were cultured for 24 h with IL-3 and the expression of RANKL (**C**), OPG (**D**), and M-CSF (**E**) mRNA was evaluated by real-time PCR. (**F**) RANKL protein expression was evaluated by Western blotting at 48 h. (**G**) Relative intensities were calculated by densitometry using ImageJ software. Data are representative of three (A and B) and two (F) independent experiments. Bar graphs are expressed as the average of three (C–E) or two (G) independent experiments. $*p < 0.05$, $**p < 0.01$, IL-3 versus untreated controls.

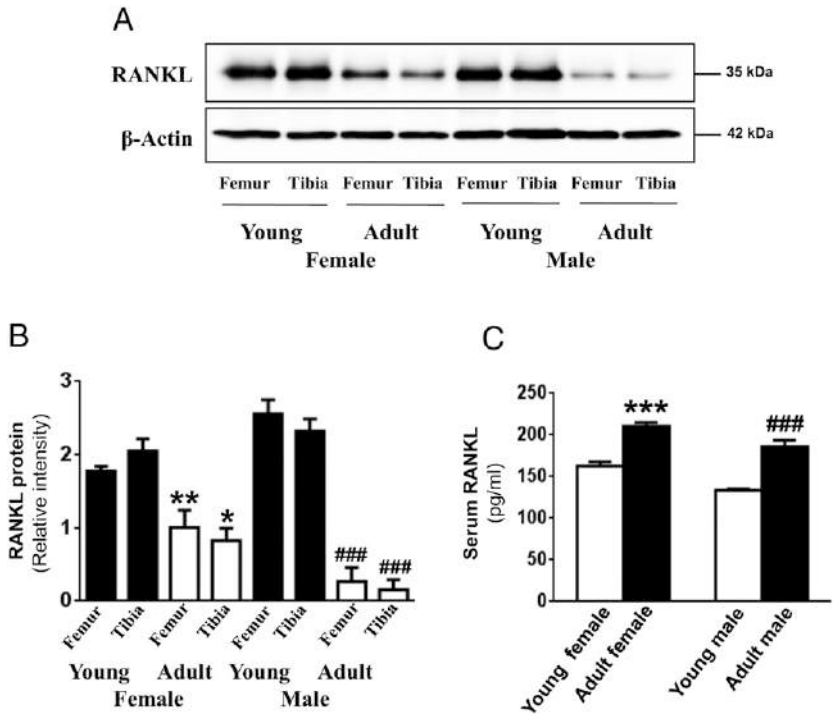

FIGURE 7. In vivo age-associated changes in RANKL expression. Changes in bone tissue and serum-specific RANKL expression were analyzed by Western blotting (**A**) and ELISA (**C**), respectively, in female and male young mice (3 mo old) and adult mice (1 y old). (**B**) Relative intensity of RANKL measured by densitometry using ImageJ software. Data are expressed as mean ± SEM ($n = 5$). $^{*}p < 0.05$, $^{**}p < 0.01$, $^{***}p < 0.001$, adult versus young female mice. $^{\#\#\#}p < 0.001$, adult versus young male mice.

with IL-3 for 30 min, and analysis of STAT5 translocation was evaluated by immunofluorescence. IL-3 increases the translocation of pSTAT5 into the nucleus (Fig. 6B). Thus, IL-3 activates STAT5 via JAK2 and also induces its translocation into nucleus.

RANKL expression is regulated by JAK2/STAT5a in mammary epithelial cells (11), and IL-3 increases phosphorylation of both isoforms of STAT5 (42, 43). To further investigate which isoform of STAT5 play a prominent role in IL-3 regulation of RANKL expression, we used AT-MSCs isolated from wild-type, STAT5a, and STAT5b knockout mice. AT-MSCs were selected over osteoblasts or bone marrow MSCs because of ease of isolation and expansion as a homogeneous population that differentiates into osteoblasts (33). AT-MSCs showed all characteristics of MSCs and the differentiation potential into functional osteoblasts (data not shown). AT-MSCs were cultured for 24 or 48 h with IL-3 and the expression of RANKL was analyzed at both the gene and protein levels, and OPG was analyzed at the mRNA level. IL-3 significantly increased RANKL expression at the mRNA (Fig. 6C) and protein (Fig. 6F, 6G) levels in wild-type AT-MSCs, but it showed no change in RANKL expression in STAT5a knockout AT-MSCs. IL-3–treated cells from STAT5b knockout mice showed no effect on RANKL expression at the mRNA level (Fig. 6C) but significantly decreased RANKL expression at the protein level (Fig. 6F, 6G). No comparative effect of IL-3 was observed on OPG and M-CSF expression between wild-type, STAT5a, and STAT5b knockout mice (Fig. 6D, 6E). Our results indicate that STAT5a plays a crucial role in IL-3 regulation of RANKL expression.

In vivo role of IL-3 in regulation of the RANKL/OPG ratio in adult mice

Because IL-3 regulates RANKL expression differentially in vitro in osteoblasts, we further analyzed the in vivo effect of IL-3 on RANKL and OPG modulation. We first compared RANKL and OPG expression in young and adult female and male mice. After removal of bone marrow, femur and tibia bones were used to analyze the expression of bone-specific RANKL. Serum was used to analyze the soluble RANKL. It was observed that bone-specific RANKL expression was significantly decreased in both adult female and male mice as compared with young mice (Fig. 7A). Fig. 7B represents the relative intensity of immunoblots measured by ImageJ software. We observed that serum RANKL expression was significantly increased in both adult female and male mice (Fig. 7C). These results suggested the differential regulation of RANKL expression in adult mice.

Although both female and male mice show similar changes in RANKL expression associated with bone and serum, to evaluate the role of IL-3 on RANKL, male mice were selected over female mice to avoid age-related hormonal changes. Adult male mice were injected i.p. with PBS or IL-3 (3 μg per mouse per day) for 5 d. Young mice injected with PBS were used as a control to compare the age-related changes in RANKL. Immunoblotting analysis showed a significant decrease in bone-specific RANKL in adult mice and it was markedly increased by IL-3 (Fig. 8A). Fig. 8B represents the relative quantitative analysis of immunoblots. Interestingly, IL-3 significantly decreased RANKL and increased OPG in the serum of adult mice (Fig. 8C, 8D). Furthermore, the increased RANKL/OPG ratio in adult mice was decreased by IL-3 (Fig. 8E). All of these results indicate that IL-3 helps in restoring the disturbed RANKL and OPG expression in adult mice.

Discussion

Osteoclast differentiation involves interactions between osteoblasts/stromal cells and osteoclast progenitors of hematopoietic cell lineage (1). RANKL and M-CSF, expressed by osteoblasts, and the cognate receptor RANK, present on the surface of osteoclast progenitors, play an important role in osteoblast and osteoclast interactions (7). Osteoblasts also secrete OPG that functions as a decoy receptor for RANKL and prevent the binding of RANKL to RANK that eventually inhibits osteoclast formation (18). Thus, the RANKL–RANK–OPG axis is very important for regulation of osteoclastogenesis and maintenance of bone homeostasis (44). In important skeletal diseases such as osteoporosis, osteoarthritis, and bone cancers the RANKL/OPG ratio increases (19). Many osteotropic factors including hormones and cytokines regulate osteoclastogenesis and bone resorption indirectly by modulating the expression and/or activity of RANKL,

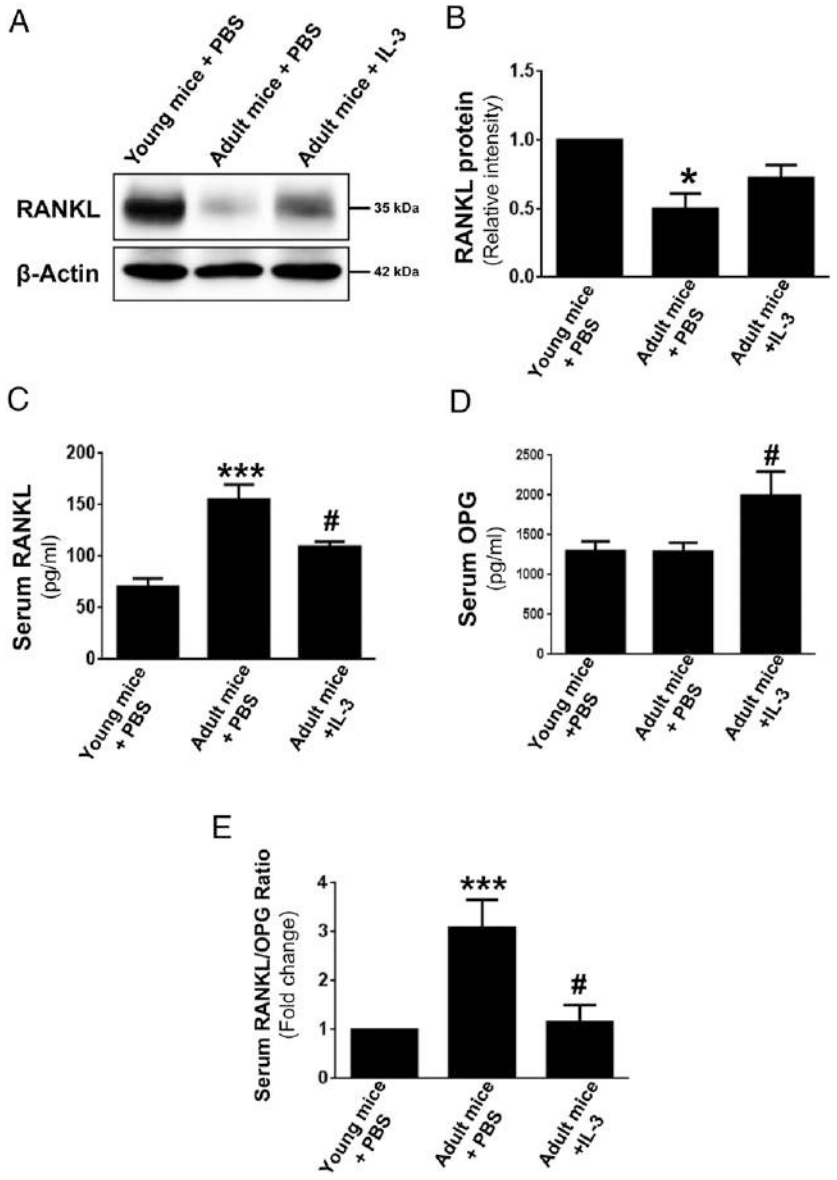

FIGURE 8. In vivo role of IL-3 on regulation RANKL/OPG ratio in adult mice. Adult male mice were injected i.p. with PBS or IL-3 (3 μg per mouse per day) for 5 d. Young mice injected with PBS were used as a control. (**A**) Changes in bone-associated RANKL expression was measured by Western blotting. (**B**) Relative intensity was calculated by densitometry using ImageJ software. Serum RANKL (**C**) and OPG (**D**) were measured by ELISA. (**E**) Serum RANKL/OPG ratio. Bar graphs are expressed as mean ± SEM ($n = 5$). $^{*}p < 0.05$, $^{***}p < 0.001$, adult versus young mice. $^{\#}p < 0.05$, IL-3 versus adult mice.

OPG, and RANK (19). We have previously shown that IL-3 is a potent inhibitor of osteoclast differentiation and pathological bone loss (25–28), and it also enhances osteoblast differentiation and bone formation from human MSCs (29). IL-3 inhibits osteoclast differentiation by direct action on osteoclast precursors and also inhibits RANK expression at the posttranslational level (45). Thus, IL-3 has a novel role in inhibition of pathological bone loss and enhancement of bone formation. However, it is not yet known whether IL-3 regulates crosstalk between osteoblasts and osteoclasts and has any indirect role in regulating bone loss. In the present study, we evaluated both the in vitro and in vivo roles of IL-3 on the regulation of RANKL and OPG expression.

IL-3 significantly increased RANKL expression in calvarial osteoblasts at both the transcriptional and translational levels. Our results are in agreement with a previous report that indicated that IL-3 increases RANKL expression in human basophils (46). However, this increase in RANKL expression by IL-3 was not sufficient to induce the formation of multinuclear mature osteoclasts. IL-3 showed no effect on both gene and protein expression of OPG in osteoblasts. We further analyzed the role of IL-3 on functional forms of RANKL. RANKL has two different functional forms, one membrane anchored and another a secreted soluble form (35). Surprisingly, IL-3 differentially regulates two functional forms of RANKL. IL-3 increases the expression of membrane-bound RANKL and simultaneously downregulates the secretion of soluble RANKL. Our comparative studies showed that both vitamin D_3 and IL-3 significantly stimulated RANKL expression at transcriptional and translational levels. However, only vitamin D_3 significantly stimulated secretion of soluble RANKL. These results indicate that vitamin D_3, a well-known stimulator of osteoclast formation in coculture, stimulates osteoclastogenesis by inducing both membrane and soluble RANKL, whereas IL-3 stimulates membrane-bound RANKL and inhibits soluble RANKL.

Similar to many other transmembrane proteins, RANKL undergoes proteolysis and it is released from its plasma membrane by a process called ectodomain shedding (36, 37). The ectodomain shedding is a highly regulated process that affects biological and pathological significance of many transmembrane proteins. For example, cytokine TNF-α and epidermal growth factor exert their paracrine and endocrine effects only after ectodomain shedding (47, 48). Similar to other members of the TNF family, such as TNF-α (47) and Fas ligand (49), the membrane-bound RANKL is converted to a soluble form through ectodomain shedding (34,

35). Members of the ADAM family such as ADAM10, ADAM17, and ADAM19 exhibit RANKL shedding activity (36). MMP3 and MMP14 also cleave RANKL, although the cleavage site for MMP14 differs from others (38, 39). In our study, IL-3 significantly decreases the expression of ADAM10, ADAM17, ADAM19, and MMP3 at the mRNA level. This reduction in ADAMs in osteoblasts may be involved in downregulation of soluble RANKL by IL-3. Therefore, our results indicate that despite increasing membrane-bound RANKL on osteoblasts, IL-3 does not induce mature osteoclast formation and this effect of IL-3 may be due to a decrease in soluble RANKL.

Among various signaling pathways, JAK2/STAT5 is the predominant pathway activated by IL-3 (42). Activated JAK2 stimulates the phosphorylation of STAT5, which is translocated to the nucleus and binds to specific DNA elements to activate transcription of target genes (50). In our system, IL-3 activates the JAK2/STAT5 pathway by increasing the phosphorylation of STAT5a and STAT5b. It has been reported that STAT5a increases RANKL expression by interaction of STAT5a to the RANKL promoter; however, STAT5b showed no role in the regulation of RANKL (11). Our knockout mice studies also support this finding where we observed that IL-3–activated RANKL expression was regulated by STAT5a; however, the role of STAT5b in the regulation of RANKL expression is not yet clear.

Aging is one of the risk factor for bone loss, although the underlying mechanisms are not yet clear. Similar to other pathological conditions such as osteoporosis and multiple myeloma, RANKL and OPG are also important in the regulation of age-associated bone homeostasis (51–53). Interestingly, we observed that as age increases the RANKL associated with bone decreases dramatically in both male and female mice. This observation raises an interesting question that if RANKL is associated with the development of age-related osteoporosis, then how does the bone become more prone to fracture even after expressing less bone-specific RANKL? We further observed that RANKL expression in serum increased significantly in adult mice. Cumulatively, these observations suggest that although RANKL is important for bone metabolism, it plays a different role at different locations. Our studies show that in bone, a basal level of RANKL is required to maintain its structural integrity, and increased serum RANKL may cause development of bone pathology. Our in vitro results showed that IL-3 regulates the two functional forms of RANKL differently. Considering membrane-bound RANKL as bone specific and serum RANKL as soluble, our in vivo analysis demonstrate that IL-3 helps in maintaining RANKL expression in bone and serum by enhancing bone-specific RANKL and decreasing serum RANKL.

In contrast to RANKL, OPG expression does not change in serum of adult mice. In adult age, increased RANKL expression with no change in OPG level indicates that the increased RANKL/OPG ratio in serum might be responsible for the development of an osteopenia-like bone phenotype at this stage. Our results indicate that the significant increase in OPG expression by IL-3 in the serum of adult mice helps to maintain the RANKL/OPG ratio.

In conclusion, our study shows that IL-3 differentially regulates two functional forms of RANKL under both in vitro and in vivo conditions. In our previous studies, we showed that IL-3 inhibits osteoclast formation in a direct manner (25–28). In the present study we confirmed that IL-3 does not induce multinuclear osteoclast formation in an indirect manner due to differential regulation of RANKL. As reported earlier, IL-3 has a dual role in regulation of bone metabolism, that is, it inhibits osteoclastogenesis (25–28) and stimulates osteoblast differentiation (29). IL-3 also prevents pathological bone loss in murine models of inflammatory arthritis (27, 54, 55). Present in vivo studies show that IL-3 not only reduces the elevated circulatory RANKL expression in adult mice, but it also significantly increases OPG. Thus, IL-3 helps in maintaining RANKL and OPG expression in adult mice. Thus, the direct inhibition of osteoclast formation, the inability to induce osteoclastogenesis in a indirect manner, and downregulation of soluble RANKL by IL-3 indicate its potential in treatment of bone loss associated with aging and important skeletal disorders that develop due to increased serum RANKL (51–53).

Acknowledgments

We thank Satish T. Pote for technical assistance.

Disclosures

The authors have no financial conflicts of interest.

References

1. Suda, T., N. Takahashi, N. Udagawa, E. Jimi, M. T. Gillespie, and T. J. Martin. 1999. Modulation of osteoclast differentiation and function by the new members of the tumor necrosis factor receptor and ligand families. *Endocr. Rev.* 20: 345–357.
2. Tanaka, S., N. Takahashi, N. Udagawa, T. Tamura, T. Akatsu, E. R. Stanley, T. Kurokawa, and T. Suda. 1993. Macrophage colony-stimulating factor is indispensable for both proliferation and differentiation of osteoclast progenitors. *J. Clin. Invest.* 91: 257–263.
3. Yoshida, H., S. Hayashi, T. Kunisada, M. Ogawa, S. Nishikawa, H. Okamura, T. Sudo, L. D. Shultz, and S. Nishikawa. 1990. The murine mutation osteopetrosis is in the coding region of the macrophage colony stimulating factor gene. *Nature* 345: 442–444.
4. Yasuda, H., N. Shima, N. Nakagawa, K. Yamaguchi, M. Kinosaki, S. Mochizuki, A. Tomoyasu, K. Yano, M. Goto, A. Murakami, et al. 1998. Osteoclast differentiation factor is a ligand for osteoprotegerin/osteoclastogenesis-inhibitory factor and is identical to TRANCE/RANKL. *Proc. Natl. Acad. Sci. USA* 95: 3597–3602.
5. Wong, B. R., J. Rho, J. Arron, E. Robinson, J. Orlinick, M. Chao, S. Kalachikov, E. Cayani, F. S. Bartlett, III, W. N. Frankel, et al. 1997. TRANCE is a novel ligand of the tumor necrosis factor receptor family that activates c-Jun N-terminal kinase in T cells. *J. Biol. Chem.* 272: 25190–25194.
6. Anderson, D. M., E. Maraskovsky, W. L. Billingsley, W. C. Dougall, M. E. Tometsko, E. R. Roux, M. C. Teepe, R. F. DuBose, D. Cosman, and L. Galibert. 1997. A homologue of the TNF receptor and its ligand enhance T-cell growth and dendritic-cell function. *Nature* 390: 175–179.
7. Lacey, D. L., E. Timms, H. L. Tan, M. J. Kelley, C. R. Dunstan, T. Burgess, R. Elliott, A. Colombero, G. Elliott, S. Scully, et al. 1998. Osteoprotegerin ligand is a cytokine that regulates osteoclast differentiation and activation. *Cell* 93: 165–176.
8. Loser, K., A. Mehling, S. Loeser, J. Apelt, A. Kuhn, S. Grabbe, T. Schwarz, J. M. Penninger, and S. Beissert. 2006. Epidermal RANKL controls regulatory T-cell numbers via activation of dendritic cells. *Nat. Med.* 12: 1372–1379.
9. Croucher, P. I., C. M. Shipman, J. Lippitt, M. Perry, K. Asosingh, A. Hijzen, A. C. Brabbs, E. J. van Beek, I. Holen, T. M. Skerry, et al. 2001. Osteoprotegerin inhibits the development of osteolytic bone disease in multiple myeloma. *Blood* 98: 3534–3540.
10. Choi, Y., K. M. Woo, S. H. Ko, Y. J. Lee, S. J. Park, H. M. Kim, and B. S. Kwon. 2001. Osteoclastogenesis is enhanced by activated B cells but suppressed by activated $CD8^+$ T cells. *Eur. J. Immunol.* 31: 2179–2188.
11. Srivastava, S., M. Matsuda, Z. Hou, J. P. Bailey, R. Kitazawa, M. P. Herbst, and N. D. Horseman. 2003. Receptor activator of NF-κB ligand induction via Jak2 and Stat5a in mammary epithelial cells. *J. Biol. Chem.* 278: 46171–46178.
12. Ishida, A., N. Fujita, R. Kitazawa, and T. Tsuruo. 2002. Transforming growth factor-β induces expression of receptor activator of NF-κB ligand in vascular endothelial cells derived from bone. *J. Biol. Chem.* 277: 26217–26224.
13. Huang, L., Y. Y. Cheng, L. T. Chow, M. H. Zheng, and S. M. Kumta. 2002. Tumour cells produce receptor activator of NF-κB ligand (RANKL) in skeletal metastases. *J. Clin. Pathol.* 55: 877–878.
14. Shimamura, M., H. Nakagami, M. K. Osako, H. Kurinami, H. Koriyama, P. Zhengda, H. Tomioka, A. Tenma, K. Wakayama, and R. Morishita. 2014. OPG/RANKL/RANK axis is a critical inflammatory signaling system in ischemic brain in mice. *Proc. Natl. Acad. Sci. USA* 111: 8191–8196.
15. Hsu, H., D. L. Lacey, C. R. Dunstan, I. Solovyev, A. Colombero, E. Timms, H. L. Tan, G. Elliott, M. J. Kelley, I. Sarosi, et al. 1999. Tumor necrosis factor receptor family member RANK mediates osteoclast differentiation and activation induced by osteoprotegerin ligand. *Proc. Natl. Acad. Sci. USA* 96: 3540–3545.
16. Levaot, N., A. Ottolenghi, M. Mann, G. Guterman-Ram, Z. Kam, and B. Geiger. 2015. Osteoclast fusion is initiated by a small subset of RANKL-stimulated monocyte progenitors, which can fuse to RANKL-unstimulated progenitors. *Bone* 79: 21–28.
17. Jimi, E., S. Akiyama, T. Tsurukai, N. Okahashi, K. Kobayashi, N. Udagawa, T. Nishihara, N. Takahashi, and T. Suda. 1999. Osteoclast differentiation factor acts as a multifunctional regulator in murine osteoclast differentiation and function. *J. Immunol.* 163: 434–442.

18. Simonet, W. S., D. L. Lacey, C. R. Dunstan, M. Kelley, M. S. Chang, R. Lüthy, H. Q. Nguyen, S. Wooden, L. Bennett, T. Boone, et al. 1997. Osteoprotegerin: a novel secreted protein involved in the regulation of bone density. *Cell* 89: 309–319.
19. Theoleyre, S., Y. Wittrant, S. K. Tat, Y. Fortun, F. Redini, and D. Heymann. 2004. The molecular triad OPG/RANK/RANKL: involvement in the orchestration of pathophysiological bone remodeling. *Cytokine Growth Factor Rev.* 15: 457–475.
20. Kostenuik, P. J., and V. Shalhoub. 2001. Osteoprotegerin: a physiological and pharmacological inhibitor of bone resorption. *Curr. Pharm. Des.* 7: 613–635.
21. Lee, S. K., and J. A. Lorenzo. 1999. Parathyroid hormone stimulates TRANCE and inhibits osteoprotegerin messenger ribonucleic acid expression in murine bone marrow cultures: correlation with osteoclast-like cell formation. *Endocrinology* 140: 3552–3561.
22. Onyia, J. E., R. R. Miles, X. Yang, D. L. Halladay, J. Hale, A. Glasebrook, D. McClure, G. Seno, L. Churgay, S. Chandrasekhar, and T. J. Martin. 2000. In vivo demonstration that human parathyroid hormone 1–38 inhibits the expression of osteoprotegerin in bone with the kinetics of an immediate early gene. *J. Bone Miner. Res.* 15: 863–871.
23. Lorenzo, J., M. Horowitz, and Y. Choi. 2008. Osteoimmunology: interactions of the bone and immune system. *Endocr. Rev.* 29: 403–440.
24. Schrader, J. W. 2003. Interleukin-3. In *The Cytokine Handbook.* A. W. Thomson, and M. T. Lotze, eds. Academic Press, London, U.K. p. 201–225.
25. Khapli, S. M., L. S. Mangashetti, S. D. Yogesha, and M. R. Wani. 2003. IL-3 acts directly on osteoclast precursors and irreversibly inhibits receptor activator of NF-κB ligand-induced osteoclast differentiation by diverting the cells to macrophage lineage. *J. Immunol.* 171: 142–151.
26. Yogesha, S. D., S. M. Khapli, and M. R. Wani. 2005. Interleukin-3 and granulocyte-macrophage colony-stimulating factor inhibits tumor necrosis factor (TNF)-α-induced osteoclast differentiation by down-regulation of expression of TNF receptors 1 and 2. *J. Biol. Chem.* 280: 11759–11769.
27. Yogesha, S. D., S. M. Khapli, R. K. Srivastava, L. S. Mangashetti, S. T. Pote, G. C. Mishra, and M. R. Wani. 2009. IL-3 inhibits TNF-α-induced bone resorption and prevents inflammatory arthritis. *J. Immunol.* 182: 361–370.
28. Gupta, N., A. P. Barhanpurkar, G. B. Tomar, R. K. Srivastava, S. Kour, S. T. Pote, G. C. Mishra, and M. R. Wani. 2010. IL-3 inhibits human osteoclastogenesis and bone resorption through downregulation of c-Fms and diverts the cells to dendritic cell lineage. *J. Immunol.* 185: 2261–2272.
29. Barhanpurkar, A. P., N. Gupta, R. K. Srivastava, G. B. Tomar, S. P. Naik, S. R. Joshi, S. T. Pote, G. C. Mishra, and M. R. Wani. 2012. IL-3 promotes osteoblast differentiation and bone formation in human mesenchymal stem cells. *Biochem. Biophys. Res. Commun.* 418: 669–675.
30. Boyce, B. F., and L. Xing. 2008. Functions of RANKL/RANK/OPG in bone modeling and remodeling. *Arch. Biochem. Biophys.* 473: 139–146.
31. Jonason, J. H., and R. J. O'Keefe. 2014. Isolation and culture of neonatal mouse calvarial osteoblasts. *Methods Mol. Biol.* 1130: 295–305.
32. Itzstein, C., and R. J. van 't Hof. 2012. Osteoclast formation in mouse co-cultures. *Methods Mol. Biol.* 816: 177–186.
33. Garimella, M. G., S. Kour, V. Piprode, M. Mittal, A. Kumar, L. Rani, S. T. Pote, G. C. Mishra, N. Chattopadhyay, and M. R. Wani. 2015. Adipose-derived mesenchymal stem cells prevent systemic bone loss in collagen-induced arthritis. *J. Immunol.* 195: 5136–5148.
34. Lum, L., B. R. Wong, R. Josien, J. D. Becherer, H. Erdjument-Bromage, J. Schlöndorff, P. Tempst, Y. Choi, and C. P. Blobel. 1999. Evidence for a role of a tumor necrosis factor-α (TNF-α)-converting enzyme-like protease in shedding of TRANCE, a TNF family member involved in osteoclastogenesis and dendritic cell survival. *J. Biol. Chem.* 274: 13613–13618.
35. Nakashima, T., Y. Kobayashi, S. Yamasaki, A. Kawakami, K. Eguchi, H. Sasaki, and H. Sakai. 2000. Protein expression and functional difference of membrane-bound and soluble receptor activator of NF-κB ligand: modulation of the expression by osteotropic factors and cytokines. *Biochem. Biophys. Res. Commun.* 275: 768–775.
36. Chesneau, V., J. D. Becherer, Y. Zheng, H. Erdjument-Bromage, P. Tempst, and C. P. Blobel. 2003. Catalytic properties of ADAM19. *J. Biol. Chem.* 278: 22331–22340.
37. Schlöndorff, J., L. Lum, and C. P. Blobel. 2001. Biochemical and pharmacological criteria define two shedding activities for TRANCE/OPGL that are distinct from the tumor necrosis factor α convertase. *J. Biol. Chem.* 276: 14665–14674.
38. Lynch, C. C., A. Hikosaka, H. B. Acuff, M. D. Martin, N. Kawai, R. K. Singh, T. C. Vargo-Gogola, J. L. Begtrup, T. E. Peterson, B. Fingleton, et al. 2005. MMP-7 promotes prostate cancer-induced osteolysis via the solubilization of RANKL. *Cancer Cell* 7: 485–496.
39. Hikita, A., I. Yana, H. Wakeyama, M. Nakamura, Y. Kadono, Y. Oshima, K. Nakamura, M. Seiki, and S. Tanaka. 2006. Negative regulation of osteoclastogenesis by ectodomain shedding of receptor activator of NF-κB ligand. *J. Biol. Chem.* 281: 36846–36855.
40. Pircher, T. J., H. Petersen, J. A. Gustafsson, and L. A. Haldosén. 1999. Extracellular signal-regulated kinase (ERK) interacts with signal transducer and activator of transcription (STAT) 5a. *Mol. Endocrinol.* 13: 555–565.
41. Bromberg, J., and J. E. Darnell, Jr. 2000. The role of STATs in transcriptional control and their impact on cellular function. *Oncogene* 19: 2468–2473.
42. Natarajan, C., S. Sriram, G. Muthian, and J. J. Bright. 2004. Signaling through JAK2-STAT5 pathway is essential for IL-3-induced activation of microglia. *Glia* 45: 188–196.
43. Mui, A. L., H. Wakao, A. M. O'Farrell, N. Harada, and A. Miyajima. 1995. Interleukin-3, granulocyte-macrophage colony stimulating factor and interleukin-5 transduce signals through two STAT5 homologs. *EMBO J.* 14: 1166–1175.
44. Yasuda, H., N. Shima, N. Nakagawa, S. I. Mochizuki, K. Yano, N. Fujise, Y. Sato, M. Goto, K. Yamaguchi, M. Kuriyama, et al. 1998. Identity of osteoclastogenesis inhibitory factor (OCIF) and osteoprotegerin (OPG): a mechanism by which OPG/OCIF inhibits osteoclastogenesis in vitro. *Endocrinology* 139: 1329–1337.
45. Khapli, S. M., G. B. Tomar, A. P. Barhanpurkar, N. Gupta, S. D. Yogesha, S. T. Pote, and M. R. Wani. 2010. Irreversible inhibition of RANK expression as a possible mechanism for IL-3 inhibition of RANKL-induced osteoclastogenesis. *Biochem. Biophys. Res. Commun.* 399: 688–693.
46. Poli, C., J. C. Martin, C. Braudeau, G. Bériou, C. Hémont, C. Charrier, S. Guérin, M. Heslan, and R. Josien. 2015. Receptor activating NF-κB ligand (RANKL) is a constitutive intracellular protein in resting human basophils and is strongly induced on their surface by interleukin 3. *Immunobiology* 220: 692–700.
47. Black, R. A., C. T. Rauch, C. J. Kozlosky, J. J. Peschon, J. L. Slack, M. F. Wolfson, B. J. Castner, K. L. Stocking, P. Reddy, S. Srinivasan, et al. 1997. A metalloproteinase disintegrin that releases tumour-necrosis factor-α from cells. *Nature* 385: 729–733.
48. Harris, R. C., E. Chung, and R. J. Coffey. 2003. EGF receptor ligands. *Exp. Cell Res.* 284: 2–13.
49. Schneider, P., N. Holler, J. L. Bodmer, M. Hahne, K. Frei, A. Fontana, and J. Tschopp. 1998. Conversion of membrane-bound Fas(CD95) ligand to its soluble form is associated with downregulation of its proapoptotic activity and loss of liver toxicity. *J. Exp. Med.* 187: 1205–1213.
50. Ihle, J. N. 1996. STATs: signal transducers and activators of transcription. *Cell* 84: 331–334.
51. Grimaud, E., L. Soubigou, S. Couillaud, P. Coipeau, A. Moreau, N. Passuti, F. Gouin, F. Redini, and D. Heymann. 2003. Receptor activator of nuclear factor kappaB ligand (RANKL)/osteoprotegerin (OPG) ratio is increased in severe osteolysis. *Am. J. Pathol.* 163: 2021–2031.
52. Terpos, E., R. Szydlo, J. F. Apperley, E. Hatjiharissi, M. Politou, J. Meletis, N. Viniou, X. Yataganas, J. M. Goldman, and A. Rahemtulla. 2003. Soluble receptor activator of nuclear factor κB ligand-osteoprotegerin ratio predicts survival in multiple myeloma: proposal for a novel prognostic index. *Blood* 102: 1064–1069.
53. Ominsky, M. S., X. Li, F. J. Asuncion, M. Barrero, K. S. Warmington, D. Dwyer, M. Stolina, Z. Geng, M. Grisanti, H.-L. Tan, et al. 2008. RANKL inhibition with osteoprotegerin increases bone strength by improving cortical and trabecular bone architecture in ovariectomized rats. *J. Bone Miner. Res.* 23: 672–682.
54. Srivastava, R. K., G. B. Tomar, A. P. Barhanpurkar, N. Gupta, S. T. Pote, G. C. Mishra, and M. R. Wani. 2011. IL-3 attenuates collagen-induced arthritis by modulating the development of Foxp3^{+} regulatory T cells. *J. Immunol.* 186: 2262–2272.
55. Kour, S., M. G. Garimella, D. A. Shiroor, S. T. Mhaske, S. R. Joshi, K. Singh, S. Pal, M. Mittal, H. B. Krishnan, N. Chattopadhyay, et al. 2016. IL-3 decreases cartilage degeneration by downregulating matrix metalloproteinases and reduces joint destruction in osteoarthritic mice. *J. Immunol.* 196: 5024–5035.